ELSEVIER

Neurobiology of Disease

www.elsevier.com/locate/ynbdi
Neurobiology of Disease 29 (2008) 336–353

CD40L disruption enhances Aβ vaccine-mediated reduction of cerebral amyloidosis while minimizing cerebral amyloid angiopathy and inflammation

D. Obregon,[a,1] H. Hou,[a,1] Y. Bai,[a,1] W.V. Nikolic,[a] T. Mori,[a,c] Deyan Luo,[a] J. Zeng,[a] J. Ehrhart,[a] F. Fernandez,[a] D. Morgan,[b] B. Giunta,[a] T. Town,[a,d,*,2] and J. Tan[a,b,c,*]

[a]*Neuroimmunology Laboratory, Institute for Research in Psychiatry, Department of Psychiatry and Behavioral Medicine, USA*
[b]*Department of Molecular Pharmacology and Physiology, University of South Florida, 12901 Bruce B. Downs Blvd, Tampa, FL 33613, USA*
[c]*Institute of Medical Science, Saitama Medical School, 1981 Kamoda, Kawagoe, Saitama 350-8550, Japan*
[d]*Department of Immunobiology, Yale University School of Medicine, 300 Cedar Street, New Haven, CT 06520-8011, USA*

Received 29 May 2007; revised 31 August 2007; accepted 19 September 2007
Available online 16 October 2007

Amyloid-β (Aβ) immunization efficiently reduces amyloid plaque load and memory impairment in transgenic mouse models of Alzheimer's disease (AD). Active Aβ immunization has also yielded favorable results in a subset of AD patients. However, a small percentage of patients developed severe aseptic meningoencephalitis associated with brain inflammation and infiltration of T-cells. We have shown that blocking the CD40–CD40 ligand (L) interaction mitigates Aβ-induced inflammatory responses and enhances Aβ clearance. Here, we utilized genetic and pharmacologic approaches to test whether CD40–CD40L blockade could enhance the efficacy of $A\beta_{1-42}$ immunization, while limiting potentially damaging inflammatory responses. We show that genetic or pharmacologic interruption of the CD40–CD40L interaction enhanced $A\beta_{1-42}$ immunization efficacy to reduce cerebral amyloidosis in the PSAPP and Tg2576 mouse models of AD. Potentially deleterious pro-inflammatory immune responses, cerebral amyloid angiopathy (CAA) and cerebral microhemorrhage were reduced or absent in these combined approaches. Pharmacologic blockade of CD40L decreased T-cell neurotoxicity to Aβ-producing neurons. Further reduction of cerebral amyloidosis in Aβ-immunized PSAPP mice completely deficient for CD40 occurred in the absence of Aβ immunoglobulin G (IgG) antibodies or efflux of Aβ from brain to blood, but was rather correlated with anti-inflammatory cytokine profiles and reduced plasma soluble CD40L. These results suggest CD40–CD40L blockade promotes anti-inflammatory cellular immune responses, likely resulting in promotion of microglial phagocytic activity and Aβ clearance without generation of neurotoxic Aβ-reactive T-cells. Thus, combined approaches of Aβ immunotherapy and CD40–CD40L blockade may provide for a safer and more effective Aβ vaccine.

Keywords: Alzheimer's disease; β-Amyloid; Cerebral amyloid angiopathy; Aβ immunization; CD40; CD154; CD40 ligand; CD40L; Inflammation; Microglia

Introduction

Amyloid-β (Aβ), a proteolytic product of amyloid precursor protein (APP), is a key molecule in the pathogenesis and progression of Alzheimer's disease (AD) (Blennow et al., 2006). Overproduction of soluble and aggregated Aβ species drives cerebral amyloidosis including β-amyloid plaque formation, a hallmark pathological feature of AD. Thus, methods developed to clear or prevent formation of Aβ in the brains of AD patients represent a possible treatment modality. One promising approach involves utilization of "active" Aβ immunization strategies, which produce dramatic reductions in Aβ pathology in animal studies (Schenk et al., 1999). However, a phase IIa clinical trial was abandoned after about 6% of Aβ-immunized AD patients developed aseptic meningoencephalitis (Nicoll et al., 2003; Orgogozo et al., 2003) that appeared to involve brain inflammatory reactions mediated by T-cells and microglia (Monsonego et al., 2001, 2003; Schenk and Yednock, 2002; Greenberg et al., 2003). Interestingly, a 12 month post-vaccination period analysis revealed an inverse

* Corresponding authors. Tan is to be contacted at Neuroimmunology Laboratory, Department of Psychiatry and Behavioral Medicine, University of South Florida, 3515 E. Fletcher Ave., Tampa, FL 33613. Fax: +1 813 974 1130. Town, Department of Immunobiology, Yale University School of Medicine, 300 Cedar St., P.O. Box 208011, New Haven, CT 06510-8011, USA. Fax: +1 203 676 5968.
E-mail addresses: terrence.town@yale.edu (T. Town), jtan@health.usf.edu (J. Tan).
[1] These authors contributed to this work equally.
[2] Present address: Maxine Dunitz Neurosurgical Institute and Department of Biomedical Sciences, Cedars-Sinai Medical Center, 8700 Beverly Blvd., Los Angeles, CA 90048, USA.

Available online on ScienceDirect (www.sciencedirect.com).

0969-9961/$ - see front matter © 2007 Elsevier Inc. All rights reserved.
doi:10.1016/j.nbd.2007.09.009

correlation between titers of amyloid plaque-reactive antibodies and rate of cognitive decline (Hock et al., 2003), suggesting clinical efficacy. Despite the discontinuation of the clinical trials, Aβ vaccination studies have continued in an effort to identify an immunization approach that is both safe and effective. Current approaches have focused on minimizing T-cell mediated inflammatory responses in effort to prevent central nervous system (CNS) invasion of auto-aggressive T-cells, while promoting Aβ antibody-mediated clearance mechanisms (Chackerian et al., 2006; Maier et al., 2006; Okura et al., 2006; Nikolic et al., 2007).

A possible avenue to both enhance Aβ clearance and down-regulate CNS inflammatory responses (including invasion of reactive T-cells) involves modulation of the CD40 receptor (CD40)–CD40 ligand (CD40L) system. CD40 is a ~45–50 kDa cell surface molecule, which is a member of the tumor necrosis factor-α (TNF-α)/nerve growth factor (NGF) receptor super-family. In the periphery, a variety of innate immune cells known as antigen-presenting cells (APCs) express CD40, including dendritic cells, B-cells, and monocytes/macrophages. In the CNS, CD40 is expressed by resident cells including microglia, neurons, and astrocytes, as well as by peripherally-derived APCs (Tan et al., 2002; Town et al., 2005). CD40L (also known as CD154) is expressed as a membrane-anchored molecule by activated T-cells and astrocytes, and can also be secreted as a smaller soluble protein (van Kooten and Banchereau, 2000). The CD40–CD40L interaction acts as an accessory co-stimulatory pathway involved in key immune cell processes including: activation, maturation/differentiation, growth/proliferation, and regulation of apoptosis (Town et al., 2001a).

We have previously shown that CD40 ligation is a molecular trigger for pro-inflammatory microglial activation in response to Aβ peptides (Tan et al., 1999). Further, genetic or pharmacologic blockade of the CD40–CD40L interaction reduces β-amyloid pathology in the brains of transgenic mouse models of AD (Tan et al., 1999; 2002). Increased CD40 and CD40L immunoreactivity has been found in and around β-amyloid plaques in the AD brain (Togo et al., 2000; Calingasan et al., 2002), further suggesting that CD40–CD40L interaction may contribute to Aβ/β-amyloid plaque pathology.

Recently, the CD40–CD40L interaction was determined to play a central role in promoting and maintaining dendritic cell APC phenotype during infections (Straw et al., 2003). In the context of CNS immunity, the CD40–CD40L interaction is required for microglial maturation into functional APCs (Ponomarev et al., 2006). We have recently shown that CD40L treatment of primary cultures of microglia inhibits phagocytosis of Aβ antibody opsonized, as well as non-opsonized Aβ species (Townsend et al., 2005). Associated with reduced Aβ phagocytic capacity, CD40L treatment up-regulated cell surface markers indicative of an APC phenotype including CD45, CD86, MHC II, and promoted the release of pro-inflammatory molecules including interleukin (IL)-1β and TNF-α (Townsend et al., 2005). Thus, the CD40–CD40L interaction may act as a molecular switch necessary to drive pro-inflammatory microglial APC phenotype maturation at the cost of reducing phagocytosis (Townsend et al., 2005; Ponomarev et al., 2006). Finally blockade of the CD40–CD40L system down-regulates T-cell/microglia-mediated neuronal injury in the context of experimental autoimmune encephalitis (EAE) (Howard et al., 1999, 2002). Altogether, these studies suggest that blockade of the CD40–CD40L interaction could enhance Aβ vaccination-mediated Aβ clearance mechanisms, while minimizing pro-inflammatory T-cell-mediated damage in the CNS.

To investigate this hypothesis, we studied transgenic "PSAPP" mice overexpressing mutant human presenilin-1 (DeltaE9), and "Swedish" mutant human APP (APP_{Swe}), which develop AD-like pathology (Jankowsky et al., 2001). We took a genetic approach to CD40 blockade by crossing these mice with $CD40^{-/-}$ mice to yield: CD40 wild-type (PSAPP), CD40 heterozygous deficient (PSAPP/$CD40^{+/-}$), and CD40 homozygous deficient (PSAPP/$CD40^{-/-}$) animals. We then vaccinated these mice over a course of 4 months utilizing aggregated $Aβ_{1–42}$ peptide or vehicle. We also took a pharmacologic approach by administering CD40L neutralizing antibody to $Aβ_{1–42}$-vaccinated PSAPP mice. Results from both strategies showed enhanced reduction of cerebral amyloidosis as evidenced by reductions in Aβ load, β-amyloid plaque burden, and cerebral amyloid angiopathy (CAA). Moreover, we report reduced cerebral microhemorrhage and inflammatory immune responses as measured by cytokine analysis and T-cell induced neurotoxicity to Aβ producing neurons. These results were associated with inhibition of the microglial APC phenotype. Interestingly, homozygous CD40 deficient $Aβ_{1–42}$-immunized PSAPP mice displayed reduced cerebral amyloidosis in the absence of immunoglobulin G (IgG) antibodies or efflux of Aβ from brain to blood. These effects were correlated with reduced plasma CD40 ligand (CD40L) and increased anti-inflammatory cytokine levels. Altogether these data suggest that disruption of the CD40–CD40L interaction enhances $Aβ_{1–42}$-immunization mediated Aβ clearance mechanisms by promoting anti-inflammatory cellular immunity to support microglial clearance of Aβ.

Materials and methods

Reagents

Anti-human Aβ monoclonal antibody (4G8) was purchased from Signet Laboratories (Dedham, MA). $Aβ_{1–42}$ peptide was obtained from Biosource International (Camarillo, CA). $Aβ_{1–42}$ peptide was added to 0.9% saline (4 mg/mL), vortexed, and incubated for 24 h at 37 °C. This solution was aliquoted, frozen and stored at −80 °C. Immediately prior to use, $Aβ_{1–42}$ aliquots were thawed and then mixed with adjuvant or PBS at 1:1 (v/v). Complete and incomplete Freund's adjuvant were purchased from Sigma. DuoSet™ enzyme-linked ELISA kits (including TNF-α, transforming growth factor-β1 (TGF-β1), IL-1β, and IL-10) were obtained from R&D Systems (Minneapolis, MN). Purified rat anti-mouse MHC class II antibody was obtained from PharMingen (San Diego, CA). Congo red and concanavalin A (Con A) were obtained from Sigma. $Aβ_{1–40}$ and $Aβ_{1–42}$ ELISA kits were purchased from IBL-America (Minneapolis, MN). Murine IgG and HRP-conjugated goat anti-mouse IgG were obtained from Pierce Biotechnology, Inc. (Rockford, IL). Goat anti-mouse IgM peroxidase conjugate antibody (A8786) was obtained from Sigma.

Mice

Wild-type C57BL/6, PSAPP mice (APP_{Swe}, PSEN1dE9) and CD40 deficient ($CD40^{-/-}$) mice were all obtained from Jackson Laboratories (Bar Harbor, ME). We crossed $CD40^{-/-}$ mice with PSAPP mice and characterized offspring by polymerase chain reaction-based genotyping for the mutant APP construct and mutant presenilin1 (PS1) gene (to examine PSAPP status) and neomycin selection vector (to type for CD40 deficiency), followed by Western blot for brain APP and splenic CD40 protein, respectively. Animals were housed and maintained under specific pathogen-free conditions in the College of Medicine Animal

Facility at the University of South Florida, and all experiments were performed in compliance with protocols approved by the University of South Florida Institutional Animal Care and Use Committee. The animals that we studied were PSAPP/CD40$^{+/+}$, PSAPP/CD40$^{+/-}$, PSAPP/CD40$^{-/-}$, CD40$^{-/-}$, and their littermates. None of the mice studied did not developed infections or neoplasms throughout the duration of this study.

Immunization strategies

For our genetic approach to CD40–CD40L blockade, we crossed PSAPP and CD40$^{-/-}$ mice and, at 8 months of age, divided them into groups consisting of Aβ_{1-42} or vehicle (PBS)-vaccinated CD40$^{-/-}$ and wild-type mice (n=8 for each group, 4♂/4♀), or PSAPP/CD40$^{+/+}$ (PSAPP/CD40$^{+/+}$/Aβ_{1-42}, PSAPP/CD40$^{+/+}$/PBS), PSAPP/CD40$^{+/-}$ (PSAPP/CD40$^{+/-}$/Aβ_{1-42}, PSAPP/CD40$^{+/-}$/PBS), or PSAPP/CD40$^{-/-}$ (PSAPP/CD40$^{-/-}$/Aβ_{1-42}, PSAPP/CD40$^{-/-}$/PBS) mice (n=16 for each group, 8♂/8♀). Immunization of these mice was performed at regular time intervals in a similar fashion to the methods described by Schenk et al. (1999). Briefly, 8-month-old mice were injected with Aβ_{1-42} (100 μg/mouse) or PBS emulsified in monophosphoryl lipid A (detoxified endotoxin) from *S. minnesota* (MPL) and synthetic trehalose dicorynomycolate (TDM) biweekly until 9 months of age, and monthly injection with Aβ_{1-42} or PBS alone was performed thereafter.

For our pharmacologic approach to CD40–CD40L blockade, we studied 8-month-old PSAPP mice divided into five groups (n=16 for each group, 8♂/8♀) as follows: PBS-treated Aβ_{1-42} immunized PSAPP mice (PSAPP/Aβ_{1-42}/PBS), CD40L antibody-treated Aβ_{1-42} immunized PSAPP mice (PSAPP/Aβ_{1-42}/CD40L antibody), Isotype control IgG-treated Aβ_{1-42} immunized PSAPP mice (PSAPP/Aβ_{1-42}/IgG antibody), or CD40L antibody-treated non-Aβ_{1-42} immunized PSAPP mice (PSAPP/CD40L antibody). We immunized these mice with Aβ_{1-42} as described above and treated them with CD40L antibody (200 μg/mouse) based on our previous report (Tan et al., 2002). For all mice, blood samples were collected from the sub-mandibular vein just before immunization and then on a monthly basis thereafter 1–2 days prior to

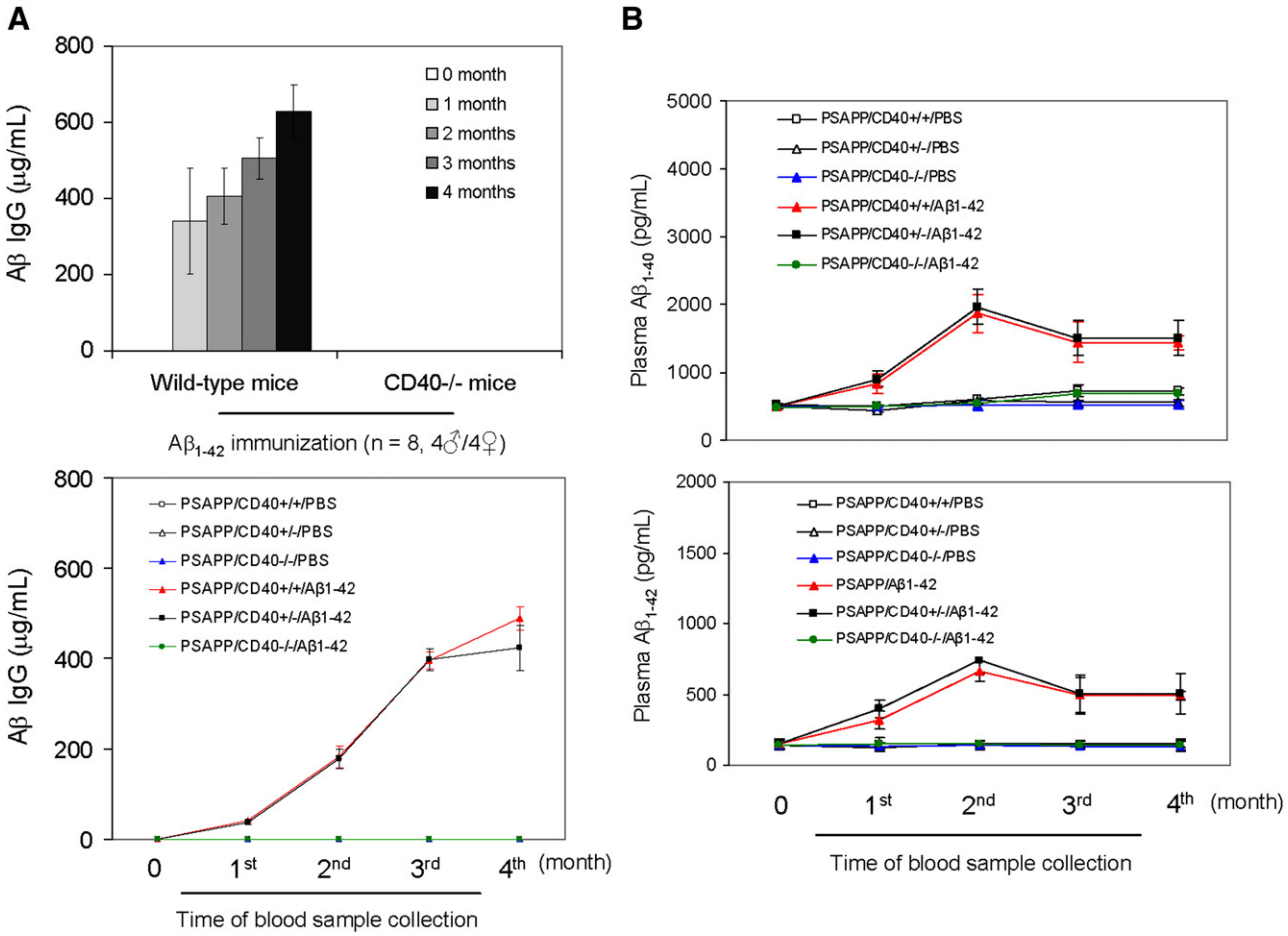

Fig. 1. Evaluation of the effects of CD40 deficiency on Aβ antibody generation and Aβ efflux in Aβ_{1-42}-immunized mice. Peripheral blood samples were collected monthly throughout the 4-month Aβ immunization course. (A) The graph shows antibody levels for wild-type vs. CD40$^{-/-}$ mice (top panel) and PSAPP mice deficient for CD40 vs. appropriate controls as indicated (bottom panel) following Aβ_{1-42} vaccination. PSAPP/CD40$^{+/+}$/Aβ_{1-42} and PSAPP/CD40$^{+/-}$/Aβ_{1-42} mice produced similar elevations in Aβ IgG antibodies, in contrast to PSAPP/CD40$^{-/-}$/Aβ_{1-42}, PSAPP/CD40$^{+/+}$/PBS, PSAPP/CD40$^{+/-}$/PBS, and PSAPP/CD40$^{-/-}$/PBS mice that produced undetectable levels of Aβ IgG antibodies. Data are presented as mean±S.D. of plasma Aβ antibodies (μg/mL). (B) Plasma Aβ_{1-40} and Aβ_{1-42} peptides were measured separately by ELISA. Data are represented as mean±S.D. of Aβ_{1-40} (top panel) or Aβ_{1-42} (bottom panel). PSAPP/CD40$^{+/+}$/Aβ_{1-42} and PSAPP/CD40$^{+/-}$/Aβ_{1-42} mice produced similar elevations in plasma Aβ_{1-40} and Aβ_{1-42}, in contrast to PSAPP/CD40$^{-/-}$/Aβ_{1-42}, PSAPP/CD40$^{+/+}$/PBS, PSAPP/CD40$^{+/-}$/PBS, and PSAPP/CD40$^{-/-}$/PBS mice that produced minimal levels of plasma Aβ_{1-40} and Aβ_{1-42}.

the succeeding monthly injection (except the final collection, which was taken 1 month after the final injection) throughout the course of immunization, and mice were sacrificed at 12 months of age.

Measurement of plasma IgG and IgM Aβ antibodies by ELISA

Aβ antibodies in individual mouse plasma and brain homogenates were measured in duplicate according to previously described methods (Maier et al., 2005). Briefly, human $A\beta_{1-42}$ peptide was coated at 1 μg/mL in 50 mM carbonate buffer, pH 9.6 (coating buffer) on 96-well immunoassay plates overnight at 4 °C. The plates were washed with 0.05% Tween 20 in PBS (washing buffer) five times and blocked with blocking buffer (PBS with 1% BSA, 5% horse serum) for 2 h at room temperature. Murine IgG or IgM was serially diluted in coating buffer (1000–0 μg/mL) to generate a standard curve. Mouse plasma and brain homogenate samples were diluted in blocking buffer at concentrations ranging from 1:400 to 1:102,400, added to the plates, and incubated for 2 h at room temperature. After 3 washes with washing buffer, a detection antibody (HRP-conjugated goat anti-mouse IgG, or HRP-conjugated goat anti-mouse IgM diluted at 1:4000), was added to the plates and incubated for 1 h at 37 °C. Following 4 washes, tetramethylbenzidine substrate was added to the plates and incubated for 15 min at room temperature. 50 microliters of stop solution (2N H_2SO_4) was added to each well of the plates. The optical density of each well was immediately determined by a microplate reader at 450 nm. Aβ antibody data are reported as μg per mL of plasma (mean ± S.D.).

Measurement of Aβ species from plasma and brain homogenates by ELISA

Mouse brains were isolated under sterile conditions on ice and placed in ice-cold lysis buffer (containing 20 mM Tris, pH 7.5, 150 mM NaCl, 1 mM EDTA, 1 mM EGTA, 1% v/v Triton X-100, 2.5 mM sodium pyrophosphate, 1 mM β-glycerolphosphate, 1 mM Na_3VO_4, 1 μg/mL leupeptin, 1 mM PMSF) as previously described (Rezai-Zadeh et al., 2005). Brains were then sonicated on ice for approximately 3 min, allowed to stand for 15 min at 4 °C, and centrifuged at 15,000 rpm for 15 min. $A\beta_{1-40}$ and $A\beta_{1-42}$ species were detected by a 2-step extraction protocol, similar to previously published methods (Johnson-Wood et al., 1997; Rezai-Zadeh et al., 2005). Detergent-soluble $A\beta_{1-40}$ and $A\beta_{1-42}$ were directly detected in plasma and brain homogenates prepared with lysis buffer described above by a 1:4 or 1:10 dilution, respectively. Total $A\beta_{1-40}$ and $A\beta_{1-42}$ species were detected by acid extraction of brain homogenates in 5 M guanidine buffer, followed by a 1:10 dilution in lysis buffer. $A\beta_{1-40}$ and $A\beta_{1-42}$ were quantified in individual samples in duplicate using $A\beta_{1-40}$ and $A\beta_{1-42}$ ELISA kits in accordance with the manufacturer's instructions (IBL-America), except that standards included 0.5 M guanidine buffer in some cases. $A\beta_{1-40}$ and $A\beta_{1-42}$ are represented as pg per mL of plasma or pg per mg of total protein (mean ± S.D.).

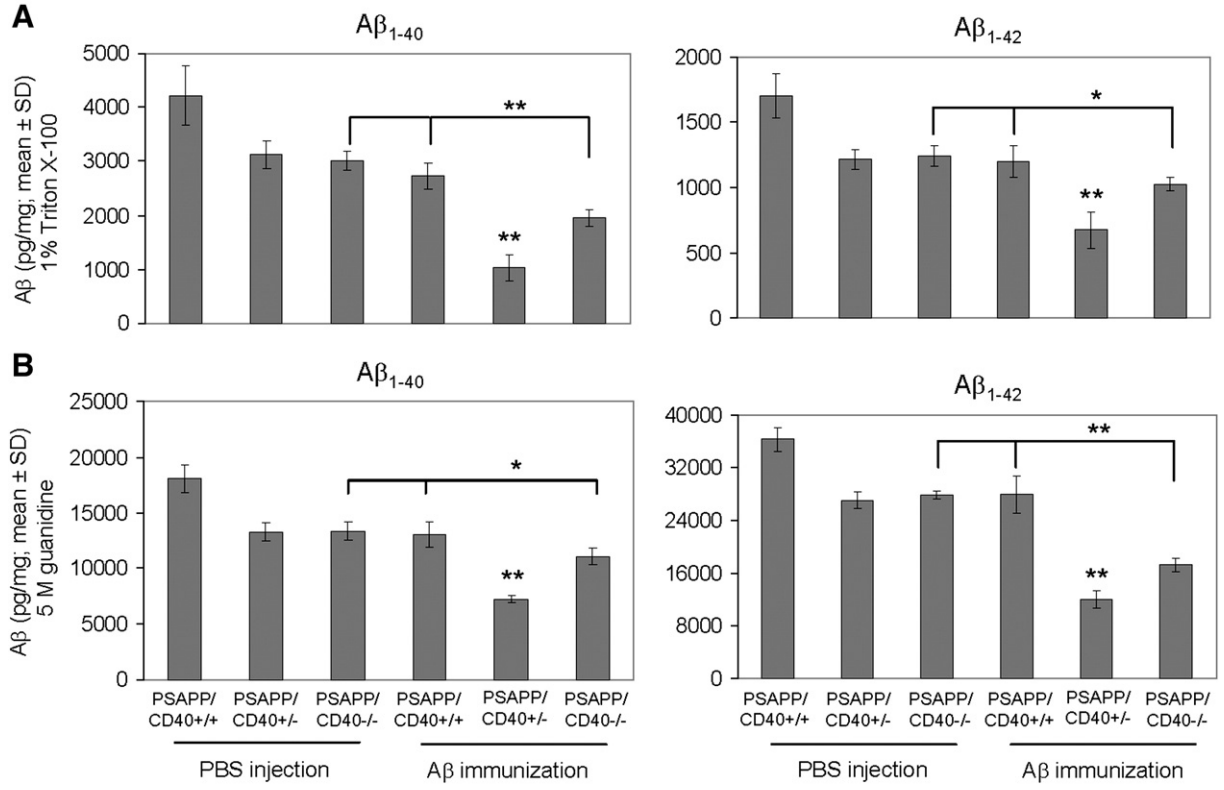

Fig. 2. Cerebral Aβ levels are significantly reduced in $A\beta_{1-42}$-immunized PSAPP mice heterozygous for CD40. Detergent-soluble $A\beta_{1-40}$ and $A\beta_{1-42}$ (A) and insoluble (5M guanidine-soluble) $A\beta_{1-40}$ and $A\beta_{1-42}$ peptides (B) were measured separately in brain homogenates by ELISA. Data are presented as mean ± S.D. of $A\beta_{1-40}$ or $A\beta_{1-42}$ (pg/mg protein).

Brain and plasma cytokine analysis

Enzyme-linked immunoabsorbance assay (ELISA) for detection of IL-1β, IL-10, TGF-β1, or TNF-α was carried out for measurement of cytokines in mouse blood plasma, or brain. Tissues were obtained at the time of sacrifice, and were diluted in PBS and assayed using the kits described above in strict accordance with the manufacturer's instruction (R&D Systems). The Bio-Rad protein assay (Bio-Rad Laboratories, Hercules, CA) was performed to measure total cellular protein from each sample prior to quantification of cytokine release

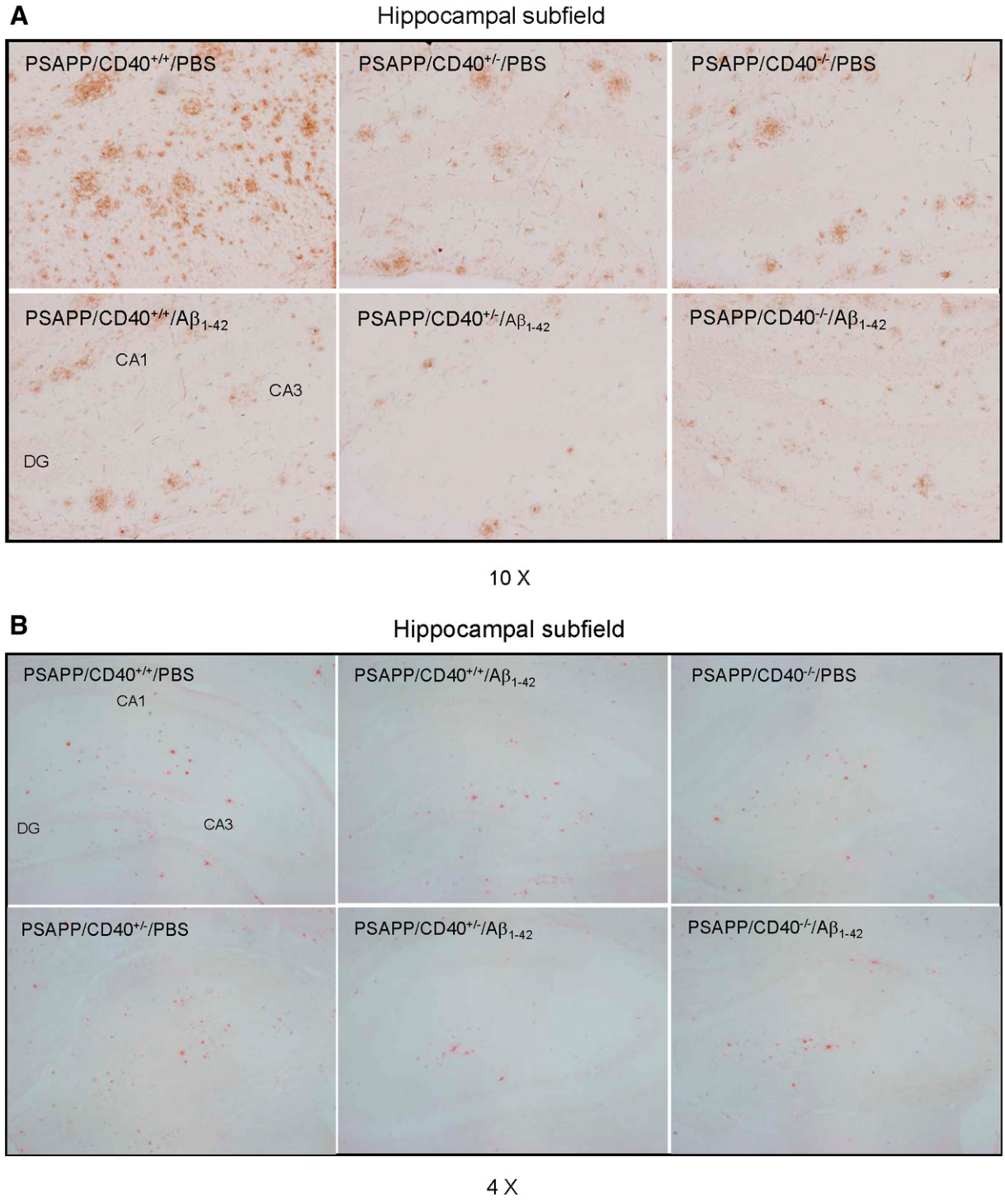

Fig. 3. β-amyloid pathology is reduced in $A\beta_{1-42}$-immunized PSAPP mice heterozygous for CD40. Mouse coronal brain sections were embedded in paraffin and stained with monoclonal human Aβ antibody (A), or were stained with congo red (B), and the hippocampus is shown. (C) Percentages [plaque area/total area; mean±S.D. with $n=16$ mice (8♂/8♀)] of Aβ antibody-immunoreactive Aβ plaques (top panel) and congo red-positive Aβ deposits (bottom panel) were calculated by quantitative image analysis for each brain region (CC/H: cingulate cortex and hippocampus; EC: entorhinal cortex) as indicated.

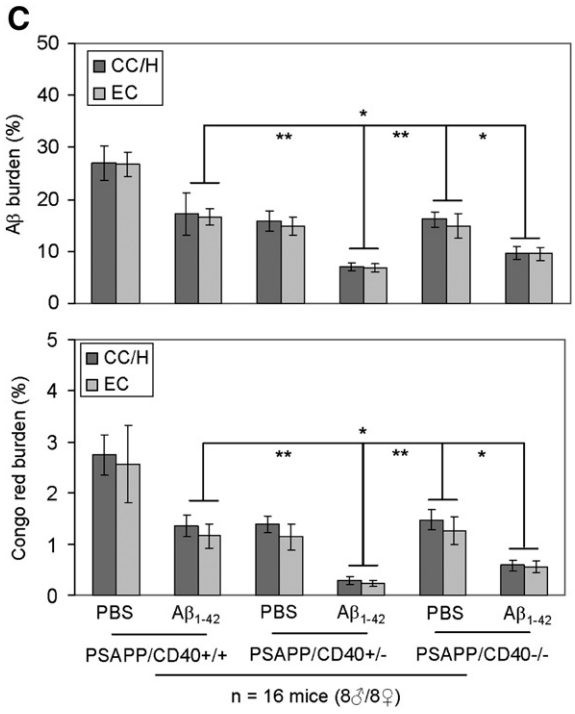

Fig. 3 (*continued*).

by ELISA, and cytokine secretion is expressed in pg/mg total protein.

Histology

Mice were anesthetized with isofluorane and transcardially perfused with ice-cold physiological saline containing heparin (10 U/mL). Brains were rapidly isolated and quartered using a mouse brain slicer (Muromachi Kikai, Tokyo, Japan). The first and second anterior quarters were homogenized for Western blot analysis, and the third and fourth posterior quarters were used for microtome or cryostat sectioning as previously described (Tan et al., 2002). Brains were then fixed in 4% paraformaldehyde in 0.9% saline at 4 °C overnight and routinely processed in paraffin in a core facility at the Department of Pathology (University of South Florida College of Medicine). Five coronal sections from each brain (5 μm thickness) were cut with a 150 μm interval. Paraffin sections were routinely deparaffinized and hydrated in a graded series of ethanol. All sections were pre-blocked for 30 min at ambient temperature with serum-free protein block (Dako Cytomation, Carpinteria, CA).

Aβ immunohistochemical staining was performed using anti-human amyloid-β antibody (clone 4G8; 1:100; Signet Laboratories) in conjunction with the VectaStain Elite ABC kit (Vector Laboratories, Burlingame, CA) coupled with the diaminobenzidine substrate. For microglia/macrophage immunostaining (MHC II, Iba1 and CD45), sections were prepared as described above. Following pre-blocking, sections were treated overnight with anti-mouse MHC II (1:500) Iba1 (1:100) or CD45 (1:500) antibodies diluted in PBS (obtained from Santa Cruz; O'Keefe et al., 2002), incubated with HRP-conjugated anti-mouse IgG, and developed. For congo red histochemistry, sections were routinely deparaffinized and rinsed in 70% (v/v) ethanol before staining with fresh-filtered 1% (w/v) congo red diluted in 70% ethanol for 5 min. These sections were rinsed three times for 5 min each in 70% ethanol, hydrated for 5 min in 0.9% saline, and mounted. β-amyloid plaques and reactive microglia were visualized using an Olympus BX-51 microscope (Olympus, Tokyo, Japan).

Quantitative image analysis was performed for 4G8 immunohistochemistry and congo red histochemistry. Images were obtained using an Olympus BX-51 microscope and digitized using an attached MagnaFire™ imaging system (Olympus, Tokyo, Japan). Briefly, images of five 5-μm sections (150 μm apart) through each anatomic region of interest (hippocampus or cortical areas) were captured and a threshold optical density was obtained

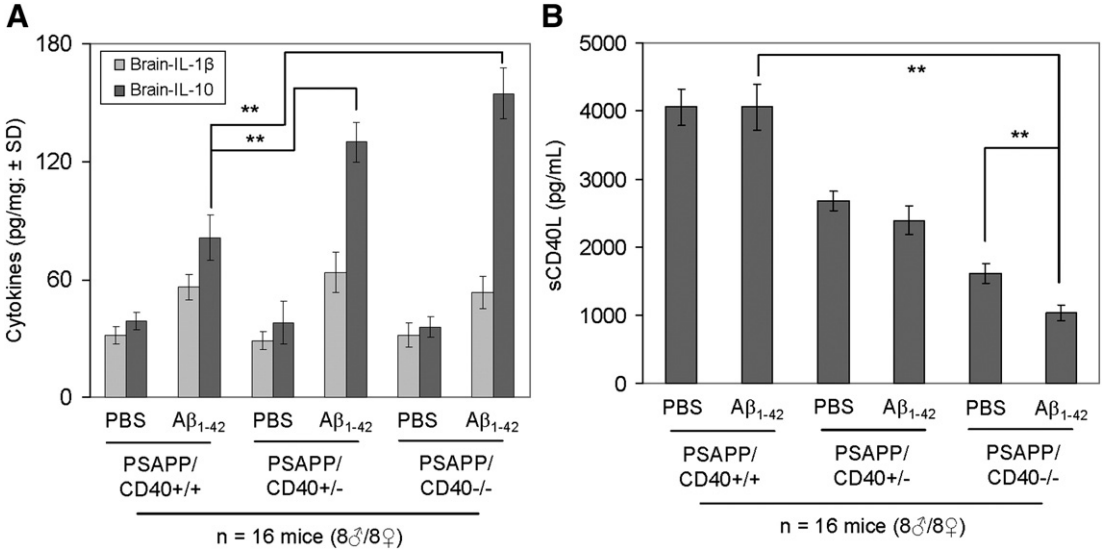

Fig. 4. PSAPP mice heterozygous or homozygously deficient for CD40 have increased anti-inflammatory IL-10 cytokine and decreased plasma soluble CD40L (sCD40L) after $A\beta_{1-42}$ vaccination. (A) ELISA analysis of cytokine levels in brain homogenates from the indicated mouse groups. Data are presented as mean ± S.D. of each cytokine (pg/mg total protein). (B) ELISA for plasma sCD40L levels in the indicated mouse groups. Data are presented as mean ± S.D. of plasma sCD40L protein (pg/mL).

that discriminated staining form background. Manual editing of each field was used to eliminate artifacts. Data are reported as percentage of immunolabeled area captured (positive pixels) divided by the full area captured (total pixels). Quantitative image analysis was performed by a single examiner (TM) blinded to sample identities.

Splenocyte cultures

Cell suspensions of splenocytes from individual mice were prepared as previously described (Town et al., 2001b, 2002) and passed in 0.5 mL aliquots into 24-well plates at 3×10^6 cells/mL. These cells were cultured for 48 h in the presence or absence of Con A (5 μg/mL), or $A\beta_{1–42}$ (20 μg/mL). Supernatants were then collected and assayed by IFN-γ, IL-2, and IL-4 cytokine ELISA kits in strict accordance with the manufacturer's instruction (R&D Systems). The Bio-Rad protein assay (Bio-Rad Laboratories, Hercules, CA) was performed to measure total cellular protein from each well prior to quantification of cytokine release by ELISA, and cytokine secretion is expressed in pg/mg total cellular protein (mean±S.D.). To verify whether stimulation of splenocytes produced any between-groups differences on cell death that might account for altered cytokine profiles, LDH release assay was carried out as described (Townsend et al., 2005) and LDH was not detected in any of the wells studied.

Aβ-specific lymphocyte neurotoxicity assay

Primary cultured neuronal cells were used as target cells in ^{51}Cr release assay for Aβ-specific lymphocyte neurotoxicity (Tan et al., 1999). We co-cultured primary neuronal cells from PSAPP mice or their littermates with $CD3^+$ T-cells (including $CD4^+$ and $CD8^+$ T-cells) isolated from primary cultures of splenocytes derived from $A\beta_{1–42}$/IgG- or $A\beta_{1–42}$/CD40L antibody-treated PSAPP mice as described above. As in our previous studies (Tan et al., 1999; Town et al., 2002), primary neuronal cells were labeled with ^{51}Cr as target cells and co-cultured with T-cells as effectors. Four-hour ^{51}Cr release assay was then carried out. Total release represents the radioactivity released after lysis of target cells with 5% Triton X-100.

Statistical analysis

All data were normally distributed; therefore, in instances of single mean comparisons, Levene's test for equality of variances followed by *t*-test for independent samples was used to assess significance. In instances of multiple mean comparisons, analysis of variance (ANOVA) was used, followed by *post-hoc* comparison using Bonferroni's method. Alpha levels were set at 0.05 for all analyses. The statistical package for the social sciences release 10.0.5 (SPSS Inc., Chicago, IL) was used for all data analysis.

Results

CD40 deficiency modulates Aβ antibody production after Aβ vaccination

It is well-established that B-cells require CD40 engagement by T-cell-derived CD40L to produce IgG antibodies in response to vaccination (Kawabe et al., 1994; Bishop and Hostager, 2003). To determine the effects of $A\beta_{1–42}$ vaccination on Aβ antibody production in the absence of CD40 expression, strain- and gender-matched CD40 deficient ($CD40^{-/-}$) and wild type mice ($n=8$ per group, 4♂/4♀) were immunized. We employed a 4-month vaccination strategy according to modified previous methods (Schenk et al., 1999) utilizing synthetic aggregated $A\beta_{1–42}$ peptide or PBS with MPL/TDM as adjuvant. Mouse plasma samples were collected monthly over this 4-month vaccination period and subjected to ELISA for measurement of Aβ antibodies. Results indicated potent Aβ IgG production in wild-type mice, whereas $CD40^{-/-}$ mice produced no detectable Aβ IgG (Fig. 1A, top panel). While $CD40^{-/-}$ mice did not produce detectable Aβ IgG, they did produce Aβ IgM that was not significantly different from wild-type mice [98.56±S.D. 7.45 vs. 86.98±S.D. 12.09 (μg/mL at 1 month after the first immunization)].

To investigate the impact of CD40 deficiency on $A\beta_{1–42}$ vaccination-induced humoral immune responses in a mouse model of AD, we vaccinated 8-month-old PSAPP mice with three CD40 genotypes (PSAPP/$CD40^{+/+}$, PSAPP/$CD40^{+/-}$, and PSAPP/$CD40^{-/-}$) with either $A\beta_{1–42}$ or vehicle (PBS). Blood samples from all mice were individually collected once monthly over the 4-month vaccination period. As expected, $A\beta_{1–42}$ vaccinated PSAPP/$CD40^{-/-}$ mice demonstrated no detectable Aβ IgG, whereas PSAPP/$CD40^{+/-}$ and PSAPP/$CD40^{+/+}$ mice produced similar increases in Aβ IgG antibodies throughout the 4-month $A\beta_{1–42}$ vaccination program (Fig. 1A, bottom panel).

Increased plasma $A\beta_{1–40}$ and $A\beta_{1–42}$ in heterozygous CD40 deficient PSAPP mice after Aβ vaccination

Activation of Aβ efflux from the CNS to the systemic circulatory system is a well-recognized clearance mechanism underlying Aβ vaccination in AD mouse models (Sigurdsson et al., 2002; Lemere et al., 2003). To determine the effect of partial or complete CD40 deficiency on activation of Aβ efflux after $A\beta_{1–42}$ vaccination, we separately measured plasma $A\beta_{1–40}$ and $A\beta_{1–42}$ species by ELISA monthly over the 4-month vaccination period. Importantly, PSAPP/$CD40^{+/-}$/$A\beta_{1–42}$ mice exhibited dramatically increased plasma $A\beta_{1–40}$ and $A\beta_{1–42}$ compared to PSAPP/$CD40^{-/-}$/$A\beta_{1–42}$ animals at the time points analyzed (Fig. 1B, $P<0.001$), pointing to a shift in Aβ load from the CNS to the systemic circulation in this group. PSAPP/$CD40^{-/-}$/$A\beta_{1–42}$ mice displayed very low levels of plasma Aβ species, similar to

Fig. 5. Peripheral and cerebral Aβ levels are reduced in $A\beta_{1–42}$-immunized PSAPP mice treated with CD40L neutralizing antibody. (A) ELISA analysis for plasma levels of $A\beta_{1–40}$ and $A\beta_{1–42}$ and Aβ antibodies. Plasma $A\beta_{1–40}$ (top panel) and $A\beta_{1–42}$ (middle panel) were measured separately by ELISA. PSAPP/$A\beta_{1–42}$/CD40L antibody and PSAPP/$A\beta_{1–42}$/IgG mice produced similar elevations in plasma $A\beta_{1–40}$ and $A\beta_{1–42}$, in contrast to PSAPP/CD40L antibody and PSAPP/PBS mice which produced minimal levels of plasma $A\beta_{1–40}$ and $A\beta_{1–42}$. Data are represented as mean±S.D. of $A\beta_{1–40}$ or $A\beta_{1–42}$ (pg/mL) in plasma. Aβ antibody levels (bottom panel) were measured by ELISA. PSAPP/$A\beta_{1–42}$/CD40L antibody and PSAPP/$A\beta_{1–42}$/IgG mice produced similar elevations in plasma Aβ IgG antibodies in contrast to PSAPP/CD40L antibody and PSAPP/PBS mice which had undetectable levels of plasma Aβ IgG antibodies. Data are presented as mean±S.D. of Aβ antibodies (μg/mL) in plasma. No significant difference in Aβ antibody levels between PSAPP/$A\beta_{1–42}$/CD40L antibody and PSAPP/$A\beta_{1–42}$/IgG mice ($P>0.05$) was observed. (B) Soluble $A\beta_{1–40}$ and $A\beta_{1–42}$ peptides (top panel) and insoluble $A\beta_{1–40}$ and $A\beta_{1–42}$ (bottom panel) in brain homogenates were measured separately by ELISA. Data are presented as mean±S.D. of $A\beta_{1–40}$ or $A\beta_{1–42}$ peptides normalized to total protein (pg/mg).

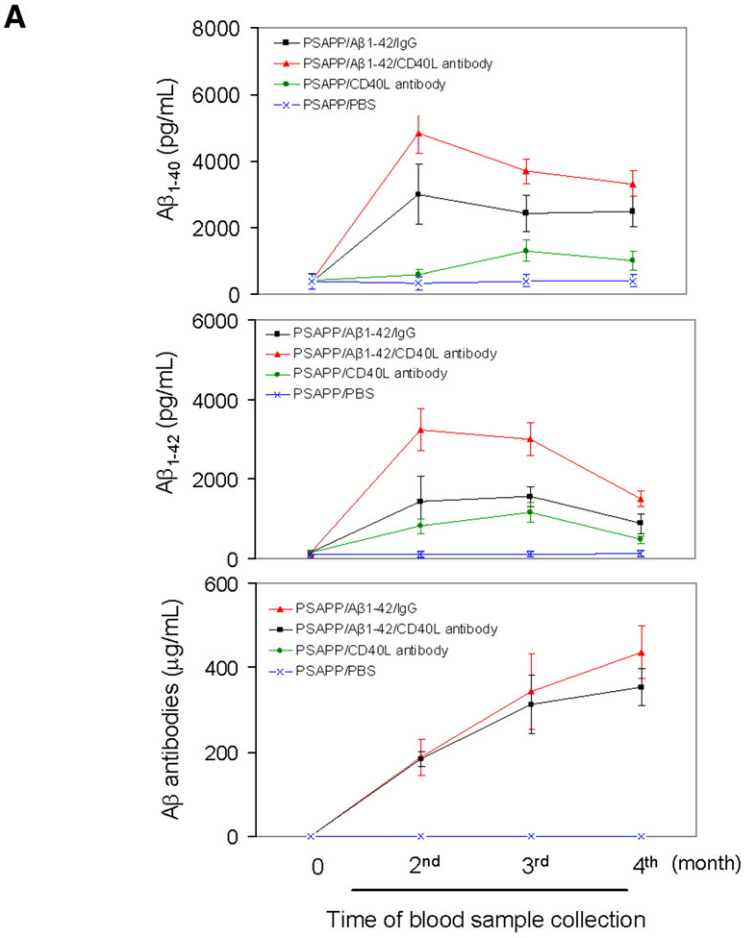
A
PSAPP/Aβ1-42/IgG
PSAPP/Aβ1-42/CD40L antibody
PSAPP/CD40L antibody
PSAPP/PBS
Aβ1-40 (pg/mL)
Aβ1-42 (pg/mL)
Aβ antibodies (μg/mL)
0
2nd
3rd
4th (month)
Time of blood sample collection

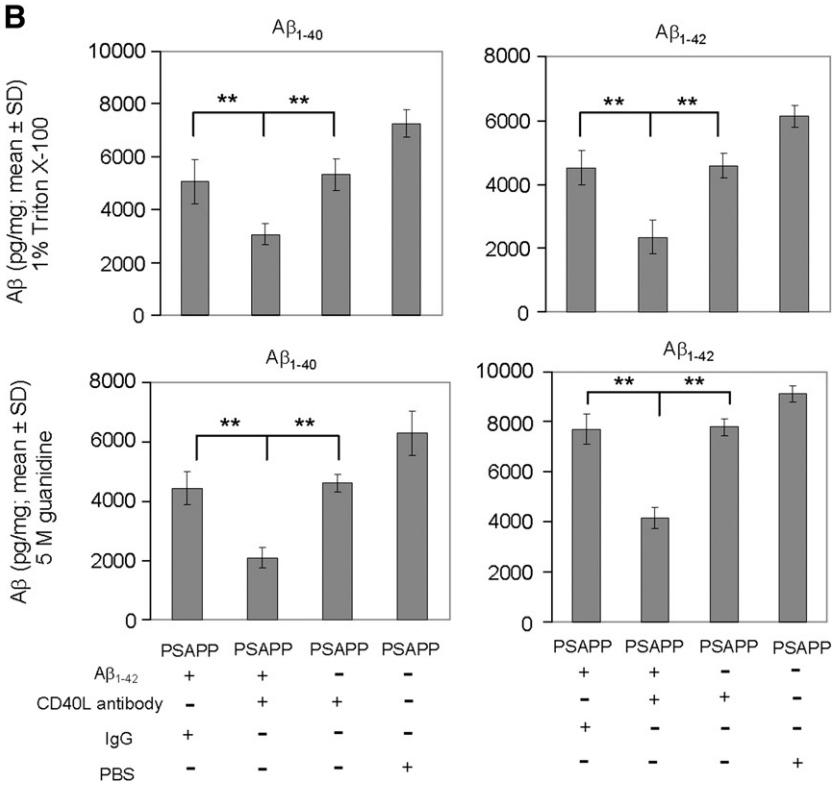
B
Aβ1-40
Aβ1-42
Aβ (pg/mg; mean ± SD)
1% Triton X-100
5 M guanidine
**
PSAPP
Aβ1-42
CD40L antibody
IgG
PBS

unvaccinated mouse groups. The lack of elevated Aβ plasma levels in PSAPP/CD40$^{-/-}$/Aβ_{1-42} mice can most likely be explained by the absence of Aβ IgG in this mouse group, as homozygous CD40 deficiency conferred absence of Aβ IgG production to either Aβ species (Fig 1A, bottom panel). Interestingly, PSAPP/CD40$^{+/-}$/Aβ_{1-42} mice displayed similarly elevated plasma levels of Aβ_{1-40} and Aβ_{1-42} when compared with the PSAPP/CD40$^{+/+}$/Aβ_{1-42} mouse group ($P>0.05$). These data further suggest that Aβ IgG production may be required for Aβ efflux from the CNS to the periphery in this vaccination paradigm.

Reduced cerebral Aβ_{1-40} and Aβ_{1-42} in heterozygous CD40 deficient PSAPP mice vaccinated with Aβ_{1-42}

As shown in Fig. 2, results revealed that Aβ_{1-42} vaccination of mice completely (PSAPP/CD40$^{-/-}$) and partially (PSAPP/CD40$^{+/-}$) deficient for CD40 yielded decreased amounts of soluble (top panels) and insoluble (bottom panels) Aβ_{1-40} and Aβ_{1-42} in brain homogenates as measured by ELISA. Most importantly, a significantly greater reduction in both soluble and insoluble Aβ_{1-40} and Aβ_{1-42} levels was evident in the PSAPP/CD40$^{+/-}$/Aβ_{1-42} group compared to either PSAPP/CD40$^{+/+}$/Aβ_{1-42} or PSAPP/CD40$^{-/-}$/Aβ_{1-42} groups (*$P<0.05$;**$P<0.001$). We further observed that β-amyloid histopathology was also markedly reduced in the PSAPP/CD40$^{+/-}$/Aβ_{1-42} group as determined by Aβ antibody immunohistochemical analysis (Fig. 3A), and congo red staining (Fig. 3B) of mouse coronal brain sections from Aβ vaccinated mice. Quantitative analysis of results revealed significantly reduced Aβ antibody and congo red-positive β-amyloid plaque burden in each brain region examined from PSAPP/CD40$^{+/-}$/Aβ_{1-42} mice as compared to either PSAPP/CD40$^{+/+}$/Aβ_{1-42} or PSAPP/CD40$^{-/-}$/Aβ_{1-42} groups (Fig. 3C, **$P<0.001$). Together, these data indicate that CD40 heterozygosity confers the greatest reduction in Aβ load in PSAPP mice when compared to all other groups following Aβ_{1-42} vaccination, and suggest that partial disruption of CD40 signaling could maximize Aβ_{1-42} vaccination efficacy.

Interestingly, Aβ plaque reduction in PSAPP/CD40$^{-/-}$/Aβ_{1-42} mice was significantly reduced when compared to PSAPP/CD40$^{+/+}$/Aβ_{1-42}, or PSAPP/CD40$^{-/-}$/PBS groups (Fig. 3C, *$P<0.05$). These data are additionally supported by ELISA analyses of both soluble and insoluble Aβ_{1-40} and Aβ_{1-42} in brain homogenates (Fig. 2), and suggest that other mechanisms besides Aβ IgG production, such as cellular immune responses, might be involved in the observed reductions of cerebral Aβ/β-amyloid in PSAPP mice after Aβ_{1-42} vaccination.

Aβ_{1-42} vaccination results in markedly increased anti-inflammatory cytokines and reduced plasma soluble CD40L in PSAPP/CD40$^{-/-}$ mice

Due to the observed lack of Aβ IgG antibodies in PSAPP/CD40$^{-/-}$ mice following Aβ_{1-42} vaccination, we wished to investigate whether cellular immune responses could be involved in reduction of cerebral Aβ/β-amyloid deposits in these animals. To test this hypothesis, we performed ELISA to examine anti-inflammatory cytokine profiles in brain homogenates from PSAPP/CD40$^{+/+}$, PSAPP/CD40$^{+/-}$, and PSAPP/CD40$^{-/-}$ mice vaccinated with either Aβ_{1-42} or vehicle (PBS). As shown in Fig. 4A, analysis of data revealed significantly (**$P<0.001$) elevated expression of brain IL-10 from either PSAPP/CD40$^{-/-}$/Aβ_{1-42} or PSAPP/CD40$^{-/+}$/Aβ_{1-42} mice compared to PSAPP/CD40$^{+/+}$/Aβ_{1-42} mice, but not for IL-1β ($P>0.05$). Moreover, we found a significant decrease in plasma soluble CD40L (sCD40L) when comparing PSAPP/CD40$^{-/-}$/Aβ_{1-42} to either PSAPP/CD40$^{+/+}$/Aβ_{1-42} or PSAPP/CD40$^{-/-}$/PBS mice (**$P<0.001$, Fig. 4B). Reduced sCD40L in PSAPP/CD40$^{-/-}$/Aβ_{1-42} compared to PSAPP/CD40$^{+/+}$/Aβ_{1-42} mice occurred in the absence of significantly different levels of Aβ IgM antibodies (data not shown). These data indicate that reduction in cerebral Aβ after Aβ_{1-42} vaccination of PSAPP/CD40$^{-/-}$ mice is associated with a rise in the anti-inflammatory cytokine IL-10 and a decrease in plasma sCD40L levels.

Neutralizing CD40L antibody increases circulating Aβ_{1-40} and Aβ_{1-42} levels and reduces cerebral amyloidosis in Aβ_{1-42} vaccinated PSAPP and Tg2576 mice

To determine whether pharmacologic inhibition of CD40–CD40L interaction might produce a similar effect as genetic disruption on enhancing Aβ_{1-42} vaccination efficacy, we administered neutralizing CD40L antibody to PSAPP mice in combination with active Aβ_{1-42} vaccination described in Materials and methods. Blood samples were individually collected from all mice at a monthly time interval. Similar to the effects observed in Aβ_{1-42} vaccinated PSAPP/CD40$^{+/-}$ mice, Aβ_{1-42} vaccinated PSAPP mice treated with CD40L antibody displayed elevations in plasma levels of Aβ_{1-40} and Aβ_{1-42} and Aβ IgG antibodies that did not significantly differ from Aβ_{1-42} vaccinated PSAPP mice injected with an isotype-matched IgG control antibody (Fig. 5A, top to bottom, respectively). The PSAPP/Aβ_{1-42}/CD40L antibody and PSAPP/Aβ_{1-42}/IgG groups produced greater plasma levels of Aβ_{1-40} and Aβ_{1-42} species and Aβ antibodies than either PSAPP mice receiving PBS or treatment with CD40L antibody alone, confirming that 1) immunization of this cohort of animals was successful and 2) neutralizing CD40L did not hamper Aβ antibody production (Fig. 5A). Additionally, no significant differences were revealed for either plasma Aβ_{1-40} and Aβ_{1-42} levels or Aβ antibodies when comparing PSAPP/Aβ_{1-42}/IgG to PSAPP/Aβ_{1-42} groups ($P>0.05$; data not shown).

We next examined the effect of neutralizing CD40L antibody on cerebral Aβ levels in PSAPP mice vaccinated with Aβ_{1-42}. ELISA analysis revealed that PSAPP/Aβ_{1-42}/CD40L antibody mice displayed significantly reduced amounts of cerebral soluble and insoluble Aβ_{1-40} and Aβ_{1-42} peptides as compared with PSAPP/Aβ_{1-42}/IgG, PSAPP/CD40L antibody, or PSAPP/PBS groups (**$P<0.001$; Fig. 5B). Furthermore, PSAPP/Aβ_{1-42}/CD40L antibody mice showed a marked reduction in cerebral Aβ deposits compared to PSAPP/Aβ_{1-42}/IgG mice or other control groups (**$P<0.001$; Figs. 6A–C). These data show additional reduction in cerebral Aβ and β-amyloid in the context of Aβ_{1-42} vaccination provided by pharmacologic blockade of CD40–CD40L interaction.

Together, these data demonstrate that disruption of the CD40–CD40L interaction by 1) a genetic approach or 2) pharmacologic depletion of available CD40L by neutralizing antibody enhances reduction of cerebral amyloidosis after Aβ_{1-42} vaccination. Recent studies have shown CAA and cerebral microhemorrhage often occur in AD mice following intraperitoneal (i.p.) active or passive Aβ vaccination (Wilcock et al., 2004, 2007). Thus, we next investigated if disruption of CD40L activity could reduce CAA following Aβ vaccination in the Tg2576 mouse model of AD. Since Tg2576 mice are known to produce CAA pathology at 15 to 20 months of age

(Christie et al., 2001; Li et al., 2003; Friedlich et al., 2004; Kim et al., 2007), we initiated i.p. injection of these mice with CD40L antibody at 12 months of age ($n=16$, 8♂/8♀) in conjunction with active $A\beta_{1-42}$ immunization using an identical procedure as described above. Four months later, we sacrificed these mice and examined CAA. As shown in Figs. 6D–E, disruption of CD40L activity by the depleting antibody not only promoted additional reduction in total congo red after $A\beta_{1-42}$ vaccination, but also further reduced vascular congo red signal. This was confirmed by statistical analysis, which revealed significant differences (**$P<0.001$) between Tg2576/$A\beta_{1-42}$/IgG

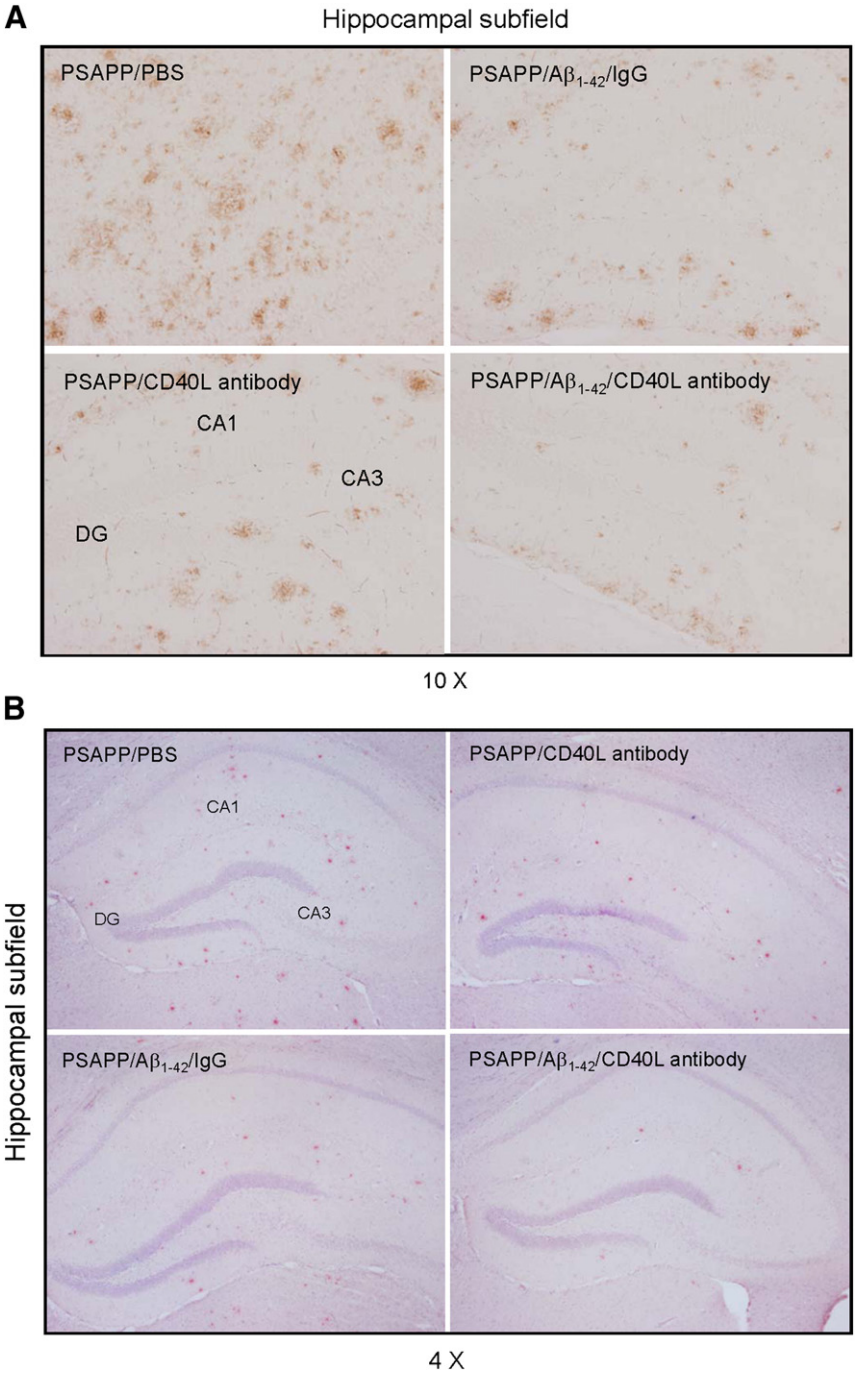

Fig. 6. Cerebral β-amyloid deposits and cerebral amyloid angiopathy are reduced in $A\beta_{1-42}$-immunized PSAPP or Tg2576 mice treated with CD40L neutralizing antibody. Mouse paraffin-embedded coronal brain sections from were stained with rabbit Pan-β-amyloid antibody (A) or with congo red (B), and the hippocampus is shown. (C) Percentages (plaque area/total area; mean±S.D.) of Aβ antibody-immunoreactive deposits (top panel) or of congo red-stained sections (bottom panel) were calculated by quantitative image analysis. (D) Tg2576 mice received $A\beta_{1-42}$ vaccination plus neutralizing CD40L antibody or isotype-matched control IgG, and brain sections were stained with congo red (hippocampus is shown). Positions of the hippocampal subfields CA1, CA3, and DG (dentate gyrus) are indicated in the upper left panel. Arrows indicate Aβ deposit-affected vessels. (E) Percentages (% of area) of congo red-stained plaques were quantified by image analysis [mean±S.D. with ($n=16$, 8♂/8♀)].

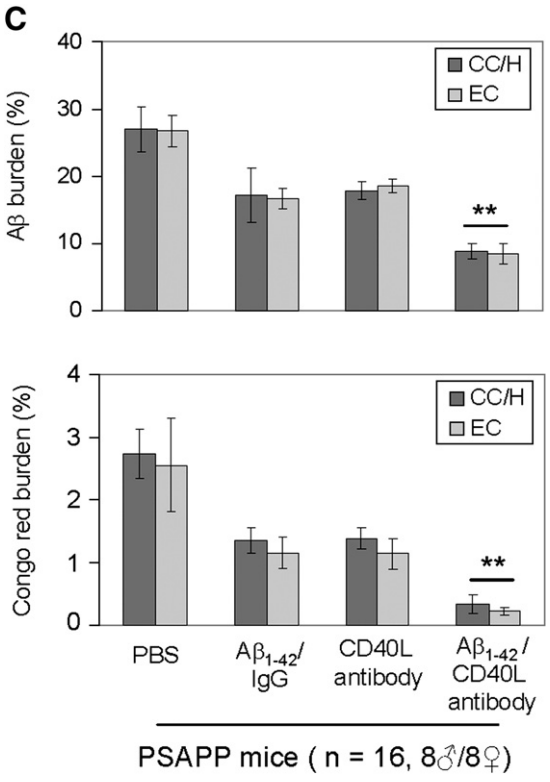

Fig. 6 (*continued*).

and Tg2576/$A\beta_{1-42}$/CD40L antibody groups for both total and vascular congo red. In addition, we also analyzed cerebral Aβ levels/β-amyloid deposits in these two groups by Aβ ELISA and immunochemistry. Similar to the effects observed in $A\beta_{1-42}$/CD40L antibody-vaccinated PSAPP mice, Tg2576 mice receiving both $A\beta_{1-42}$ immunization and depleting CD40L antibody displayed a marked decrease in cerebral soluble and insoluble $A\beta_{1-40}$ and $A\beta_{1-42}$ levels and β-amyloid load compared to $A\beta_{1-42}$-alone-immunized mice ($P<0.001$; data not shown).

CD40 pathway blockade decreases MHC II and CD45-positive microglia and increases anti-inflammatory cytokines in $A\beta_{1-42}$ immunized PSAPP mice

To evaluate the effects of CD40/CD40L blockade on pro-inflammatory APC-like microglial activation in the $A\beta_{1-42}$ vaccination paradigm, we first stained brain sections from PSAPP/$A\beta_{1-42}$/IgG and PSAPP/$A\beta_{1-42}$/CD40L antibody-treated mice with Iba1 antibody (Fig. 7A). We quantified Iba1 positive microglia/macrophages with/without the spindle-shaped morphology, as it has been previously reported that microglial cells become spindle-shaped when exposed to stimuli including LPS and Con A that promote the pro-inflammatory APC phenotype (Washington et al., 1996; Bernhardi and Nicholls, 1999). Interestingly, disruption of CD40L activity significantly reduced spindle-shaped microglia/macrophages by morphologic analysis (**$P<0.001$), but did not alter non-spindle-shaped cells (Fig. 7B). To further evaluate whether CD40L neutralization mitigated APC-like microglia, we fluorescently labeled brain sections with MHC II and CD45 antibodies. As shown in Fig. 7C, Iba1 positive microglial cells were largely positive for CD45 and MHC II in $A\beta_{1-42}$/IgG immunized PSAPP mice, but not in $A\beta_{1-42}$ and CD40L antibody co-immunized PSAPP mice. These data indicate that depletion of functional CD40L results in decreased pro-inflammatory APC-like microglial activation in PSAPP/$A\beta_{1-42}$/CD40L antibody mice. It should be noted that Iba1 immunostaining does not distinguish resident microglia from peripherally-derived monocytes that may migrate to the CNS and take up a microglial phenotype.

To further determine the consequences of this phenomenon in terms of inflammatory responses, we analyzed brain homogenates from PSAPP/$A\beta_{1-42}$/CD40L antibody, PSAPP/$A\beta_{1-42}$/IgG, and other control groups by ELISA for expression of pro-inflammatory and anti-inflammatory cytokines. Analysis of results revealed a significantly (**$P<0.001$) greater expression of anti-inflammatory TGF-β1 and IL-10 cytokines from PSAPP/$A\beta_{1-42}$/CD40L antibody mice compared to PSAPP/$A\beta_{1-42}$/IgG mice (Fig. 7D). Moreover, PSAPP/$A\beta_{1-42}$/CD40L antibody mice also produced significantly ($P<0.001$) greater expression of TGF-β1 and IL-10 when compared to other controls including PSAPP/IgG and PSAPP/$A\beta_{1-42}$/PBS mice (data not shown). No significant between-groups differences were revealed when considering TNF-α or IL-1β. These data indicate that CD40L blockade correlates with a rise in the anti-inflammatory cytokines TGF-β1 and IL-10, without affecting the pro-inflammatory cytokines TNF-α and IL-1β.

$A\beta_{1-42}$-immunized PSAPP mice treated with CD40L neutralizing antibody exhibit increases in anti-inflammatory cytokines and decreases in neurotoxic inflammatory responses in vitro

To investigate Aβ-specific T-cell immune responses after $A\beta_{1-42}$ immunization plus neutralizing CD40L antibody treatment, we established primary cultures of splenocytes from: PSAPP/$A\beta_{1-42}$/IgG, PSAPP/$A\beta_{1-42}$/CD40L antibody, PSAPP/CD40L antibody, and PSAPP/PBS mice. We then quantified key cytokines produced by activated T-cells (IFN-γ, IL-2, and IL-4) in supernatants by ELISA. Both non-specific (Con A) and specific recall stimulation of primary cultured splenocytes with $A\beta_{1-42}$ resulted in increases in the pro-inflammatory T-cell cytokines, IFN-γ and IL-2, in both PSAPP/$A\beta_{1-42}$/IgG and PSAPP/$A\beta_{1-42}$/CD40L antibody groups compared to the PSAPP/CD40L antibody group (Fig. 8A). However, these pro-inflammatory T-cell cytokines were reduced in the PSAPP/$A\beta_{1-42}$/CD40L antibody group vs. PSAPP/$A\beta_{1-42}$/IgG mice. Moreover, PSAPP/$A\beta_{1-42}$/CD40L antibody mice demonstrated an increase in the anti-inflammatory T helper type 2 cytokine IL-4 when compared to PSAPP/$A\beta_{1-42}$/IgG mice. These data indicate that disruption of CD40L activity in $A\beta_{1-42}$ vaccinated mice reduces pro-inflammatory Aβ-specific T-cell immune responses in favor of an anti-inflammatory response. One-way ANOVA followed by *post-hoc* comparison revealed significant differences when comparing PSAPP/$A\beta_{1-42}$/CD40L antibody to PSAPP/CD40L antibody or PSAPP/$A\beta_{1-42}$/IgG mouse groups for levels of each of the three cytokines (**$P<0.001$) after *in vitro* $A\beta_{1-42}$ challenge. Of note, there were significant differences within mouse groups between IL-4 and either IFN-γ or IL-2 after $A\beta_{1-42}$ recall challenge ($^{\#\#}P<0.001$). Following challenge, no significant difference in cytokine release was observed from splenocytes between PSAPP/PBS and PSAPP/$A\beta_{1-42}$/IgG control mouse groups ($P>0.05$; data not shown).

To determine whether CD40L neutralization could mitigate potentially damaging effects of Aβ-specific T-cells, we co-cultured primary neuronal cells from PSAPP mice or their littermates with $CD3^+$ T-cells (including $CD4^+$ and $CD8^+$ T-cells) isolated from

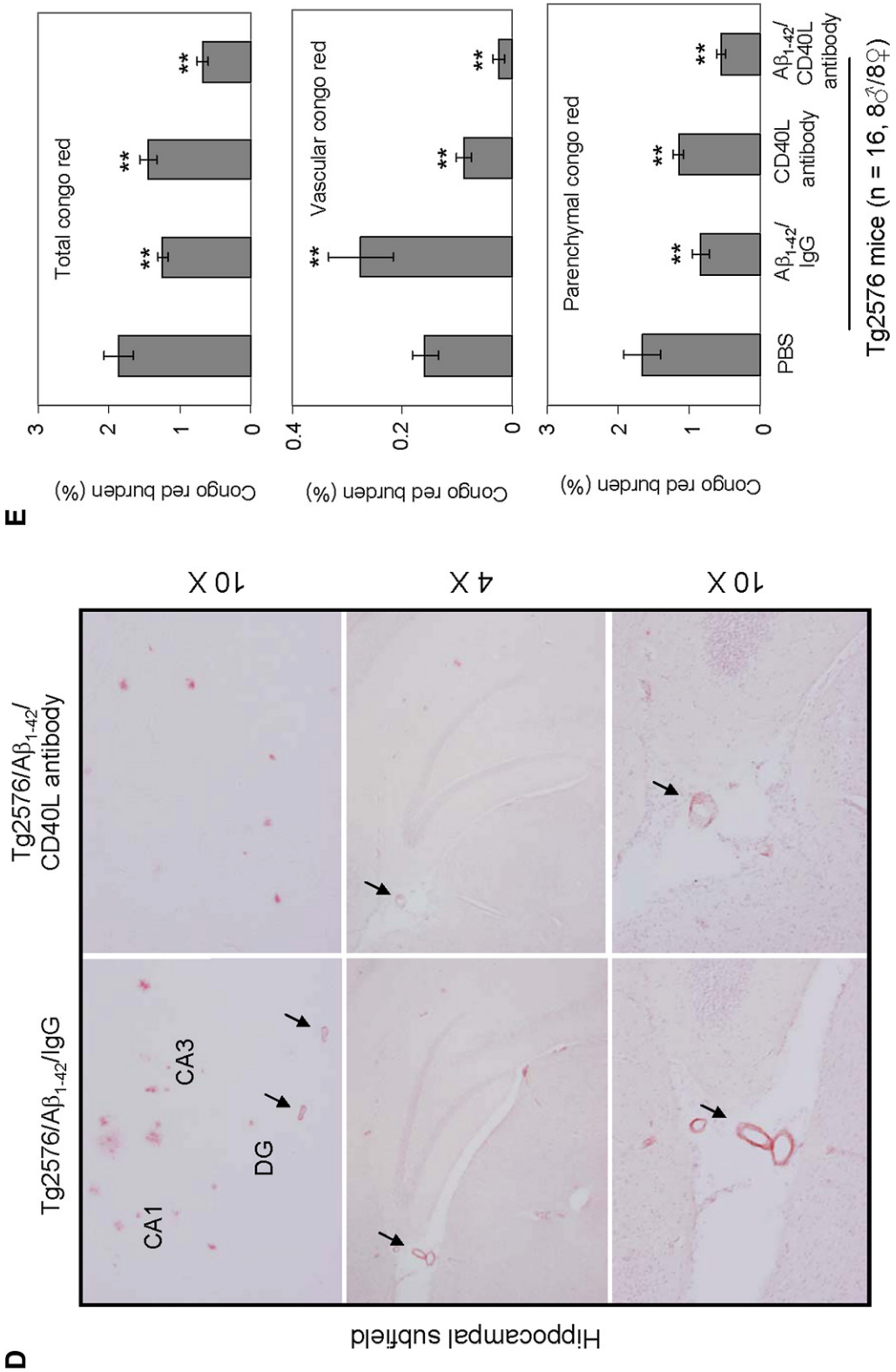

Fig. 6 (*continued*).

primary cultured splenocytes derived from PSAPP/Aβ_{1-42}/IgG or PSAPP/Aβ_{1-42}/CD40L antibody mice as described above. Per our previous reports (Tan et al., 2000, 2002; Town et al., 2002), we labeled primary neuronal cells with ^{51}Cr as target cells and co-cultured them with T-cells as effectors, and carried out 4-h ^{51}Cr release assay. ANOVA showed main effects of effector/target ratio for Aβ_{1-42} vaccinated PSAPP mouse-derived T-cells (effectors) and PSAPP mouse-derived neuronal cells (target cells) (**$P<0.001$; $n=8$ mice for PSAPP/Aβ_{1-42}/IgG and PSAPP/Aβ_{1-42}/CD40L antibody groups; $n=5$ mice for both control groups) (Fig. 8B), but not when unvaccinated PSAPP mouse-derived T-cells were used (control 1) or when control littermate (non-transgenic mouse)-derived neuronal cells (control 2) were used ($P>0.05$). ANOVA followed by *post-hoc* comparison revealed a significant difference across ratios between PSAPP/Aβ_{1-42}/IgG and PSAPP/Aβ_{1-42}/CD40L antibody T-cells (**$P<0.001$), indicating an overall decrease in percentage of cell lysis as a result of disrupting CD40L activity.

Discussion

We have previously shown the CD40–CD40L interaction enhances pro-inflammatory microglial activation triggered by cerebral Aβ deposits (Tan et al., 1999). This form of microglial activation is deleterious, as both genetic ablation of CD40L and CD40L neutralizing antibody reduce brain levels of several neurotoxic inflammatory cytokines and mitigate cerebral amyloidosis in AD mouse models (Tan et al., 2002). To establish a possible mechanism to explain these results, we previously quantified microglial phagocytic activity in CD40 deficient vs. CD40 sufficient AD mice. We observed inhibition of microglial Aβ phagocytosis upon CD40 ligation. This coincided with increased microglial co-localization of MHC class II with non-opsonized Aβ peptide. Moreover, this APC phenotype was accompanied by upregulation of pro-inflammatory Th1 cytokines such as TNF-α, IL-1β, IL-2, and IFN-γ (Townsend et al., 2005). These data suggest that CD40 pathway blockade induces "switching" of the microglial phenotype from a pro-inflammatory APC state to an anti-inflammatory, pro-phagocytic state (Townsend et al., 2005). Interestingly, brain Aβ clearance in the Aβ immunotherapy paradigm has previously been suggested to rely on microglial phagocytosis (Bard et al., 2000), and microglial Fc receptor (i.e., microglial phagocytosis of Aβ antibody-opsonized deposits) is not required for brain Aβ clearance (Das et al., 2003). Thus, we suggest that the combination of blocking the microglial CD40 pathway and Aβ immunotherapy further enhances microglial Aβ clearance.

Previous clinical investigation has revealed that active immunization with Aβ in humans confers the unacceptable risk of aseptic meningoencephalitis associated with T-cell infiltration, gliosis, and associated rise in CNS pro-inflammatory mediators (Schenk et al., 1999; Schenk and Yednock, 2002; Nicoll et al., 2003). Based on these data and our work on the CD40–CD40L association with brain Aβ levels, we investigated whether CD40 blockade could reduce cerebral Aβ deposits without the undesirable inflammatory events in the CNS.

First, we tested whether active Aβ_{1-42} vaccination of CD40 deficient mice could produce significant levels of Aβ antibodies. Consistent with the requirement of CD40 signaling for IgM to IgG class switching (Kawabe et al., 1994), homozygous CD40 deficient mice vaccinated with Aβ_{1-42} did not produce detectable Aβ IgG antibodies, but had slightly increased levels of Aβ IgM antibodies vs. wild-type controls. However, active Aβ_{1-42} vaccination of PSAPP/CD40$^{+/-}$ mice produced elevated plasma anti-Aβ IgG antibodies comparable to CD40 sufficient PSAPP mice which is

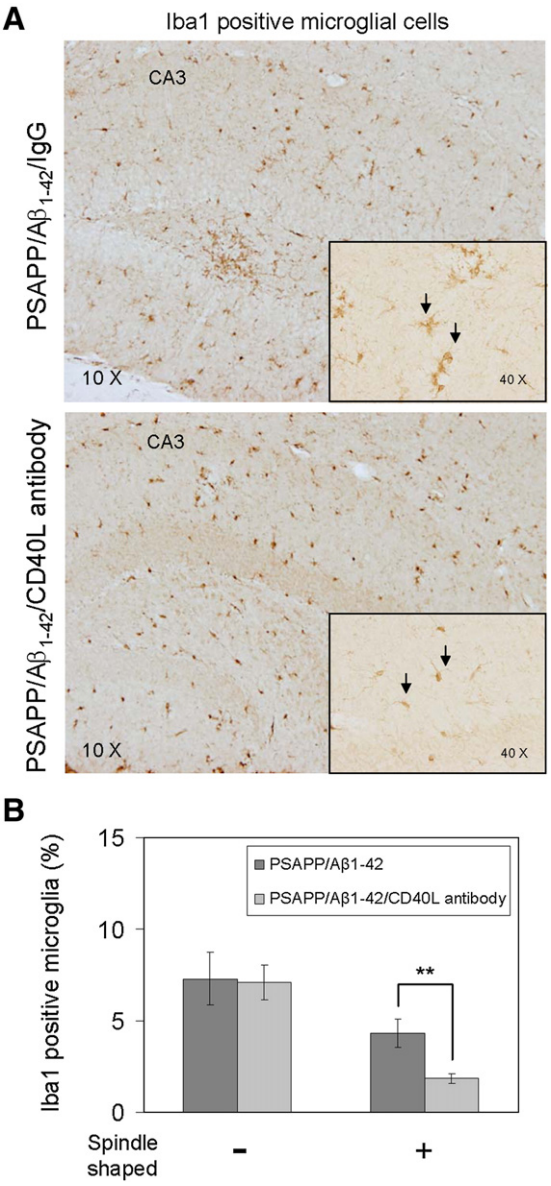

Fig. 7. CD40L blockade inhibits APC-like microglial activation and promotes anti-inflammatory cellular immunity (in Aβ_{1-42} vaccinated PSAPP mice). (A) Representative hippocampal sections from PSAPP/Aβ_{1-42}/IgG and PSAPP/Aβ_{1-42}/CD40L antibody mouse brains were stained with Iba1 antibody to illustrate both microglial load and morphology. (B) Quantitative image analysis of microglial load (Iba1 positive cells) and percentage of spindle-shaped Iba1 positive microglia is shown. (C) Representative hippocampal sections from PSAPP/Aβ_{1-42}/IgG and PSAPP/Aβ_{1-42}/CD40L antibody mouse brains were stained with Iba1 together with MHC II or CD45 antibodies to illustrate microglial load and activation status (DAPI was used as a nuclear counterstain). (D) Th1 and Th2 cytokine analysis by ELISA was conducted on mouse brain homogenates from PSAPP, PSAPP/Aβ_{1-42}/IgG and PSAPP/Aβ_{1-42}/CD40L antibody mice. Data are represented as mean ± S.D. of each cytokine in brain homogenates (pg/mg total protein) from PSAPP, PSAPP/Aβ_{1-42}/CD40L antibody or PSAPP/Aβ_{1-42}/IgG mice.

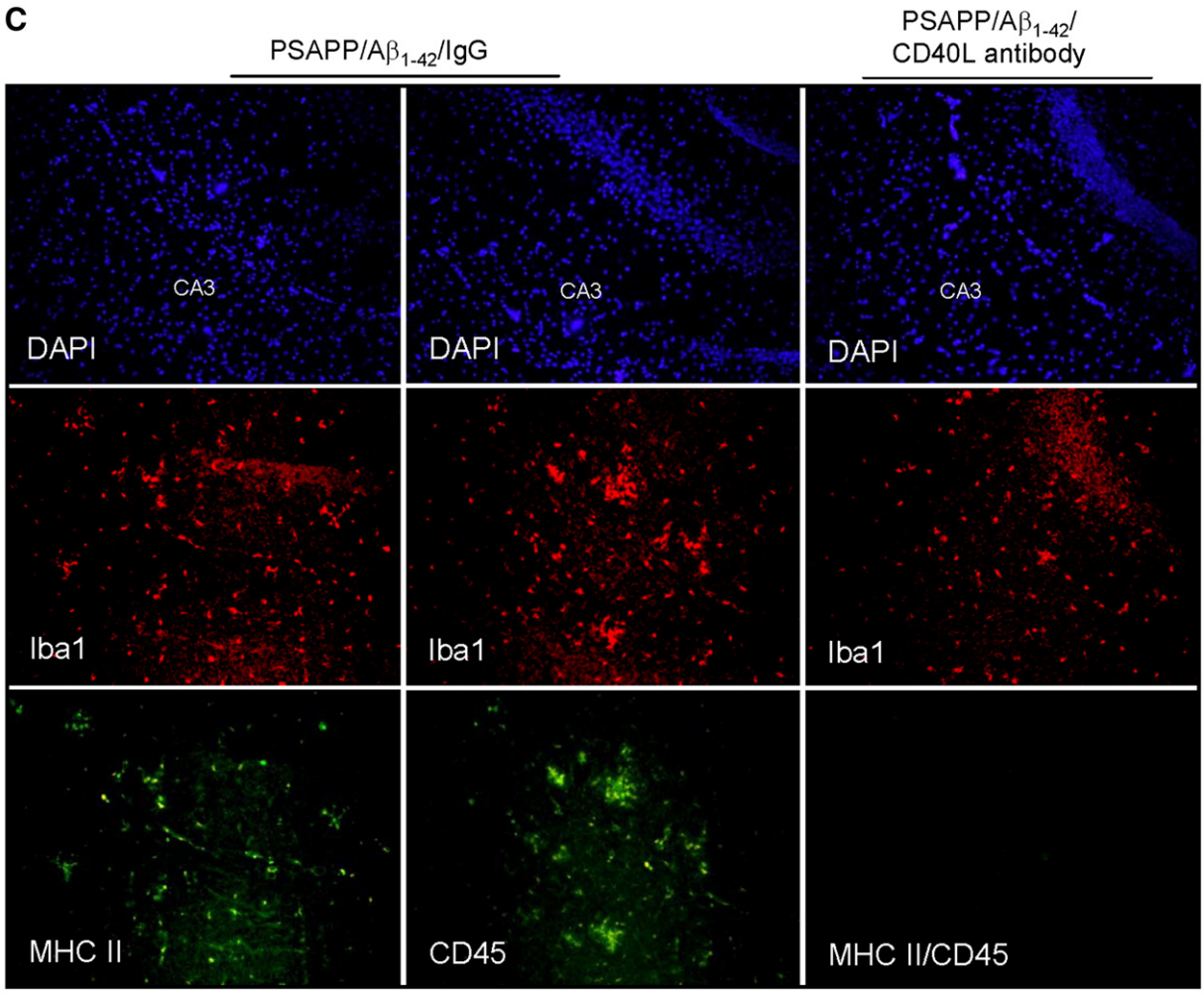

Fig. 7 (*continued*).

consistent with a gene dose-effect (Fig. 1A). Interestingly, further reduction in cerebral amyloidosis in Aβ-vaccinated PSAPP/CD40$^{-/-}$ mice occurred essentially in the absence of Aβ IgG antibodies. It is well known that the CD40 pathway is essential for antibody isotype switching from IgM to IgG, and this result suggests that the additional therapeutic benefit from blocking the CD40 pathway is independent of IgG in our system. However, given 1) the requirement of CD40 signaling for a diverse set of immunological responses and 2) that we did not use IgG deficient mice, this conclusion will require further study.

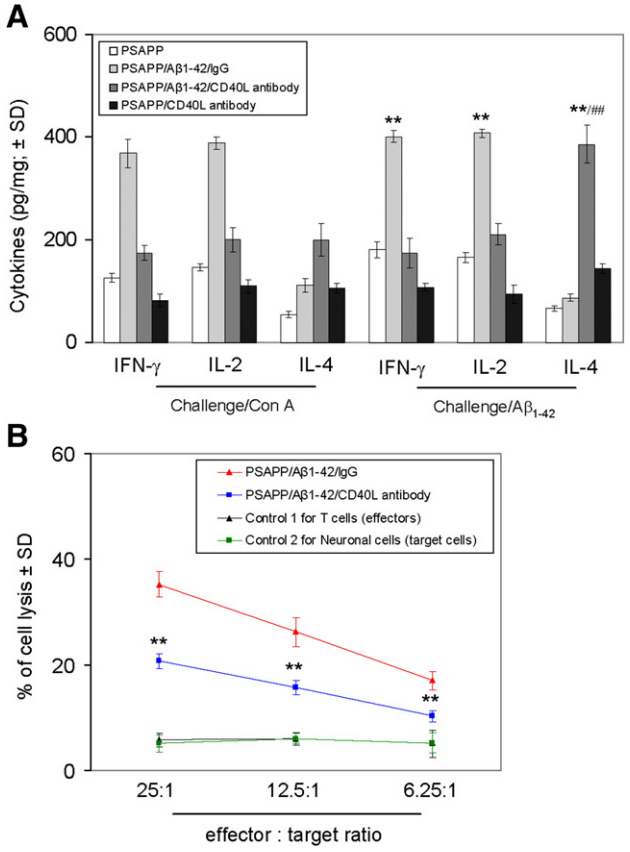

Fig. 8. Aβ-specific neurotoxic inflammatory responses are reduced in $Aβ_{1–42}$-immunized PSAPP mice deficient for CD40. (A) Splenocytes were individually isolated and cultured from mice as indicated after $Aβ_{1–42}$ immunization and either CD40L antibody treatment or IgG injection (control). These cells were stimulated with Con A (5 μg/mL) or $Aβ_{1–42}$ (20 μg/mL) for 48 h. Cultured supernatants were collected from these cells for IFN-γ, IL-2, and IL-4 cytokine analyses by ELISA. Data are represented as mean±S.D. (n=10) of each cytokine in supernatants (pg/mg total intracellular protein). (B) Aβ specific T cell-mediated neuronal cell injury was determined by ^{51}Cr release assay. Data are reported as mean ^{51}Cr release values±S.D., and n=8 for each condition presented. PSAPP/$Aβ_{1–42}$/IgG mouse group, effectors: $Aβ_{1–42}$/IgG-immunized PSAPP mouse-derived T cells; target cells: PSAPP-mouse-derived primary neuronal cells. PSAPP/$Aβ_{1–42}$/CD40L antibody mouse group, effectors: $Aβ_{1–42}$/CD40L antibody-immunized PSAPP mouse-derived T cells; target cells: PSAPP-mouse-derived primary neuronal cells. Control 1, effectors: unvaccinated PSAPP mouse-derived T cells; target cells: PSAPP mouse-derived neuronal cells. Control 2, effectors: $Aβ_{1–42}$-immunized PSAPP mouse-derived T cells; target cells: non-transgenic mouse-derived primary neuronal cells.

Next, we quantified plasma levels of $Aβ_{1–40}$ and $Aβ_{1–42}$ species across the various groups of Aβ-immunized PSAPP mice in an attempt to determine the relationship between IgG, IgM, and efflux of Aβ from the brain to the periphery. Similar elevations of plasma $Aβ_{1–40,\ 42}$ species between CD40 heterozygous deficient or CD40 sufficient PSAPP mice were observed (Fig. 1B). Thus, we suggest that Aβ IgG-mediated brain to blood efflux was operating similarly in CD40 heterozygous and CD40 sufficient PSAPP mice. By contrast, $Aβ_{1–42}$ vaccinated PSAPP/$CD40^{-/-}$ mice did not exhibit elevations in plasma $Aβ_{1–40,\ 42}$ species (Fig. 1B). This lack of elevated plasma $Aβ_{1–40,\ 42}$ correlated positively with the lack of Aβ IgG antibody production in the homozygous CD40 deficient PSAPP mice. This is consistent with a lack of brain-to-blood efflux of Aβ *via* the peripheral sink hypothesis (DeMattos et al., 2001), and suggests that a distinct mechanism is operating in these PSAPP/$CD40^{-/-}$ mice. While CD40 deficient mice do produce normal levels of Aβ IgM antibodies, no detectable elevation in peripheral Aβ was observed. This, too, is in accord with the notion that Aβ IgG is required for brain to blood efflux of Aβ (DeMattos et al., 2001). As pharmacotherapeutic "proof of principle", we administered CD40L neutralizing antibody to $Aβ_{1–42}$ vaccinated PSAPP mice, and confirmed greater reductions in cerebral amyloidosis compared to $Aβ_{1–42}$ vaccinated PSAPP mice given control IgG. This experimental approach was performed to offset the possibility that genetic ablation, in and of itself, might confer developmental changes that would result in modulation of Aβ loads.

We next went on to test T-cell specific immune responses against Aβ and found that recall stimulation of primary cultured splenocytes with $Aβ_{1–42}$ peptide resulted in reduced IFN-γ and IL-2 production in the PSAPP/$Aβ_{1–42}$/CD40L antibody mouse group compared to PSAPP/$Aβ_{1–42}$/IgG mice (Fig. 8A). Further, PSAPP/$CD40^{+/-}$/$Aβ_{1–42}$ mice exhibited an increase in the anti-inflammatory Th2 cytokine, IL-10, and produced less circulating soluble CD40L (sCD40L) compared to PSAPP/$CD40^{+/+}$/$Aβ_{1–42}$ mice (Fig. 4). Taken together, these findings suggest partial CD40 pathway inhibition reduces pro-inflammatory but increases anti-inflammatory T-cell immune responses to Aβ challenge. This is particularly attractive as these results raise the possibility that 50% pharmacological inhibition of CD40 might be of benefit in the attenuation of the pro-inflammatory meningoencephalitis associated with active Aβ vaccination in humans, while still allowing for production of Aβ IgG antibodies.

In addition to developing parenchymal Aβ deposits and associated elevated inflammatory cytokines seen in the PSAPP model, the Tg2576 mouse model of AD also develops cerebrovascular Aβ deposits not unlike cerebral amyloid angiopathy (CAA), which is observed in the majority of AD patients (Nicoll et al., 2003; Wilcock et al., 2004, 2007). To determine if reducing available CD40L might also mitigate CAA, we administered neutralizing CD40L antibody to Aβ vaccinated Tg2576 mice. Indeed, blockade of CD40L with neutralizing antibody in combination with Aβ vaccination produced the highest therapeutic effect (reduction of parenchymal Aβ) and the most minimal CAA-like pathology as measured by congo red staining (Figs. 6D–E). These results suggest CD40L antibody neutralization not only improves the cerebral amyloid reducing effect of Aβ vaccination, but also confers a reduction in CAA-like pathology in Tg2657 mice.

Previously, we showed that CD40 ligation shifts microglial response to Aβ from an anti-inflammatory phagocytic phenotype to a pro-inflammatory APC response (Town et al., 2002; Townsend et al., 2005). In accord, here we observed downregulation of microglial APC morphology *in situ* (Figs. 7A–B), and reduction in CD45 and MHC II-positive microglia from $Aβ_{1–42}$ vaccinated PSAPP mice treated with CD40L neutralizing antibody (Fig. 7C). Indeed, reduction in MHC II expression, a measure of microglial APC phenotype, correlated with elevated brain levels of anti-inflammatory Th2 cytokines TGF-β1 and IL-10 (Fig. 7D). Although NK cell-mediated activation of microglia can bypass MHC and T cell receptors to produce a vaccine immune response, infiltration of NK cells into the CNS has not been reported in the Aβ vaccination paradigm, making this less likely.

Another possibility is that so-called "anti-ergotypic" responses, defined as an immune response to the vaccine-activated host

immune cells, could play a role in enhanced efficacy of Aβ immunotherapy in conjunction with CD40 blockade. In the regard, short-term anti-ergotypic lines isolated from vaccinated Multiple Sclerosis (MS) patients demonstrate a mixed phenotype (both $CD4^+$ and $CD8^+$ cells). These cells secrete IFN-γ and TNF-α, but not TGF-β1 (Correale et al., 1997; Hellings et al., 2004). Although we can not fully rule out this mechanism in our studies of CD40 blockade enhancement of reduced cerebral amyloidosis after Aβ vaccination, it is interesting to note that our results in the CNS and in splenocytes show the converse: a reduction in IFN-γ and TNF-α, but an increase in TGF-β (Figs. 7D and 8A), suggesting the involvement of a different mechanism.

Given our previous observation that CD40 ligation induces "switching" of the microglial phenotype from a pro-phagocytic state endorsing Aβ phagocytosis to a pro-inflammatory APC state (Townsend et al., 2005), we propose that combined CD40 blockade and Aβ vaccination promotes microglial phagocytosis/clearance of Aβ from the CNS. Additionally, T-cells derived from neutralizing CD40L antibody-treated $Aβ_{1–42}$ vaccinated PSAPP mice were dramatically less neurotoxic to Aβ producing neurons *ex vivo* (Fig. 8B), suggesting further benefit afforded by combining these therapeutic approaches. However, it is worth noting that this latter result needs to be interpreted with the caveat that standard active Aβ vaccination of AD mouse models (unless modified with the addition of pertussis toxin) (Furlan et al., 2003) does not produce appreciable brain infiltrates of auto-aggressive T-cells as was observed in the active Aβ AN-1792 vaccine in AD patients (Nicoll et al., 2003; Town et al., 2005).

CD40–CD40L interaction is essential for initiating the adaptive immune response, as demonstrated by immune deficits observed in patients with mutations in the CD40 or CD40L genes. These patients develop type 1 hyper IgM immunodeficiency syndrome (HIGM1) that is characterized by recurrent bacterial and opportunistic infections (Durandy and Honjo, 2001; Fuleihan, 2001; Levy et al., 1997). Patients with homozygous mutations in the CD40 gene have a severe immunodeficiency termed HIGM3. Its clinical phenotype overlaps with that of HIGM1 and is characterized by defective generation of secondary antibodies and severe opportunistic infections (Ferrari et al., 2001; Kutukculer et al., 2003), particularly *Cryptosporidium enteritis* and *Pneumocystis carinii* pneumonia (Levy et al., 1997). Thus, complete systemic blockade of CD40–CD40L would likely have deleterious immunosuppressive side effects. For this reason, pharmacotherapy would need to be titrated such that the CD40–CD40L pathway was partially inhibited. Interestingly, as we have shown in our proof-of-concept paradigm in transgenic mice, even a 50% blockade of CD40 is enough to increase the efficacy of the Aβ vaccine on reduction of cerebral amyloidosis.

Our observations suggest that partial blockade of CD40 signaling, either by genetic or by pharmacologic means, increases the effectiveness of $Aβ_{1–42}$ vaccination by further reducing cerebral amyloidosis and simultaneously promoting anti-inflammatory cellular immune processes in the brain and in the periphery. If the benefit afforded by CD40 pathway blockade to $Aβ_{1–42}$ vaccinated AD mouse models can translate to the clinical syndrome, then pharmacotherapy aimed at reducing CD40 signaling in conjunction with Aβ vaccination may represent an approach that is both safer and more effective in humans. Future studies will be required to isolate CD40–CD40L downstream signaling involved in reduced efficacy of Aβ vaccination, as this may uncover additional targets for pharmacologic intervention.

Acknowledgments

This work is supported by grants to JT from the NIH/NINDS and NIH/NIA (AG04418). In addition, this work is supported by a NIH/NINDS supplemental grant (DO). TT is supported by an Alzheimer's Association grant and an NIH/NIA "Pathway to Independence" award (1 K99AG029726-01).

References

Bard, F., Cannon, C., Barbour, R., Burke, R.L., Games, D., Grajeda, H., Guido, T., Hu, K., Huang, J., Johnson-Wood, K., Khan, K., Kholodenko, D., Lee, M., Lieberburg, I., Motter, R., Nguyen, M., Soriano, F., Vasquez, N., Weiss, K., Welch, B., Seubert, P., Schenk, D., Yednock, T., 2000. Peripherally administered antibodies against amyloid beta-peptide enter the central nervous system and reduce pathology in a mouse model of Alzheimer disease. Nat. Med. 6 (8), 916–919.

Bernhardi, R.V., Nicholls, J.G., 1999. Transformation of leech microglial cell morphology and properties following co-culture with injured central nervous system tissue. J. Exp. Biol. 202 (Pt 6), 723–728.

Bishop, G.A., Hostager, B.S., 2003. The CD40–CD154 interaction in B cell-T cell liaisons. Cytokine Growth Factor Rev. 14, 297–309.

Blennow, K., de Leon, M.J., Zetterberg, H., 2006. Alzheimer's disease. Lancet 368, 387–403.

Calingasan, N.Y., Erdely, H.A., Altar, C.A., 2002. Identification of CD40 ligand in Alzheimer's disease and in animal models of Alzheimer's disease and brain injury. Neurobiol. Aging 23, 31–39.

Chackerian, B., Rangel, M., Hunter, Z., Peabody, D.S., 2006. Virus and virus-like particle-based immunogens for Alzheimer's disease induce antibody responses against amyloid-beta without concomitant T cell responses. Vaccine 24, 6321–6331.

Christie, R., Yamada, M., Moskowitz, M., Hyman, B., 2001. Structural and functional disruption of vascular smooth muscle cells in a transgenic mouse model of amyloid angiopathy. Am. J. Pathol. 158, 1065–1071.

Correale, J., McMillan, M., Li, S., McCarthy, K., Le, T., Weiner, L.P., 1997. Antigen presentation by autoreactive proteolipid protein peptide-specific T cell clones from chronic progressive multiple sclerosis patients: roles of co-stimulatory B7 molecules and IL-12. J. Neuroimmunol. 72, 27–43.

Das, P., Howard, V., Loosbrock, N., Dickson, D., Murphy, M.P., Golde, T.E., 2003. Amyloid-beta immunization effectively reduces amyloid deposition in FcRgamma−/− knock-out mice. J. Neurosci. 23 (24), 8532–8538.

DeMattos, R.B., Bales, K.R., Cummins, D.J., Dodart, J.C., Paul, S.M., Holtzman, D.M., 2001. Peripheral anti-A beta antibody alters CNS and plasma A beta clearance and decreases brain A beta burden in a mouse model of Alzheimer's disease. Proc. Natl. Acad. Sci. U. S. A. 98, 8850–8855.

Durandy, A., Honjo, T., 2001. Human genetic defects in class-switch recombination (hyper-IgM syndromes). Curr. Opin. Immunol. 13, 543–548 (Review).

Ferrari, S., Giliani, S., Insalaco, A., Al-Ghonaium, A., Soresina, A.R., Loubser, M., Avanzini, M.A., Marconi, M., Badolato, R., Ugazio, A.G., Levy, Y., Catalan, N., Durandy, A., Tbakhi, A., Notarangelo, L.D., Plebani, A., 2001. Mutations of CD40 gene cause an autosomal recessive form of immunodeficiency with hyper IgM. Proc. Natl. Acad. Sci. U. S. A. 98 (22), 12614–12619 (Oct 23).

Friedlich, A.L., Lee, J.Y., van Groen, T., Cherny, R.A., Volitakis, I., Cole, T.B., Palmiter, R.D., Koh, J.Y., Bush, A.I., 2004. Neuronal zinc exchange with the blood vessel wall promotes cerebral amyloid angiopathy in an animal model of Alzheimer's disease. J. Neurosci. 24, 3453–3459.

Fuleihan, R.L., 2001. The hyper IgM syndrome. Curr. Allergy Asthma Rep. 1, 445–450 (Review).

Furlan, R., Brambilla, E., Sanvito, F., Roccatagliata, L., Olivieri, S., Bergami, A., Pluchino, S., Uccelli, A., Comi, G., Martino, G., 2003.

Vaccination with amyloid-beta peptide induces autoimmune encephalomyelitis in C57/BL6 mice. Brain 126 (Pt 2), 285–291.

Greenberg, S.M., Bacskai, B.J., Hyman, B.T., 2003. Alzheimer disease's double-edged vaccine. Nat. Med. 9, 389–390.

Hellings, N., Raus, J., Stinissen, P., 2004. T-cell vaccination in multiple sclerosis: update on clinical application and mode of action. Autoimmun. Rev. 3 (4), 267–275.

Hock, C., Konietzko, U., Streffer, J.R., Tracy, J., Signorell, A., Muller-Tillmanns, B., Lemke, U., Henke, K., Moritz, E., Garcia, E., Wollmer, M.A., Umbricht, D., de Quervain, D.J., Hofmann, M., Maddalena, A., Papassotiropoulos, A., Nitsch, R.M., 2003. Antibodies against beta-amyloid slow cognitive decline in Alzheimer's disease. Neuron 38, 547–554.

Howard, L.M., Miga, A.J., Vanderlugt, C.L., Dal Canto, M.C., Laman, J.D., Noelle, R.J., Miller, S.D., 1999. Mechanisms of immunotherapeutic intervention by anti-CD40L (CD154) antibody in an animal model of multiple sclerosis. J. Clin. Invest. 103, 281–290.

Howard, L.M., Ostrovidov, S., Smith, C.E., Dal Canto, M.C., Miller, S.D., 2002. Normal Th1 development following long-term therapeutic blockade of CD154–CD40 in experimental autoimmune encephalomyelitis. J. Clin. Invest. 109, 233–241.

Jankowsky, J.L., Slunt, H.H., Ratovitski, T., Jenkins, N.A., Copeland, N.G., Borchelt, D.R., 2001. Co-expression of multiple transgenes in mouse CNS: a comparison of strategies. Biomol. Eng. 17, 157–165.

Johnson-Wood, K., Lee, M., Motter, R., Hu, K., Gordon, G., Barbour, R., Khan, K., Gordon, M., Tan, H., Games, D., Lieberburg, I., Schenk, D., Seubert, P., McConlogue, L., 1997. Amyloid precursor protein processing and A beta42 deposition in a transgenic mouse model of Alzheimer disease. Proc. Natl. Acad. Sci. U. S. A. 94, 1550–1555.

Kawabe, T., Naka, T., Yoshida, K., Tanaka, T., Fujiwara, H., Suematsu, S., Yoshida, N., Kishimoto, T., Kikutani, H., 1994. The immune responses in CD40–deficient mice: impaired immunoglobulin class switching and germinal center formation. Immunity 1, 167–178.

Kim, J., Onstead, L., Randle, S., Price, R., Smithson, L., Zwizinski, C., Dickson, D.W., Golde, T., McGowan, E., 2007. Abeta40 inhibits amyloid deposition in vivo. J. Neurosci. 27, 627–633.

Kutukculer, N., Moratto, D., Aydinok, Y., Lougaris, V., Aksoylar, S., Plebani, A., Genel, F., Notarangelo, L.D., 2003. Disseminated cryptosporidium infection in an infant with hyper-IgM syndrome caused by CD40 deficiency. J. Pediatr. 142, 194–196.

Lemere, C.A., Spooner, E.T., LaFrancois, J., Malester, B., Mori, C., Leverone, J.F., Matsuoka, Y., Taylor, J.W., DeMattos, R.B., Holtzman, D.M., Clements, J.D., Selkoe, D.J., Duff, K.E., 2003. Evidence for peripheral clearance of cerebral Abeta protein following chronic, active Abeta immunization in PSAPP mice. Neurobiol. Dis. 14, 10–18.

Levy, J., Espanol-Boren, T., Thomas, C., Fischer, A., Tovo, P., Bordigoni, P., Resnick, I., Fasth, A., Baer, M., Gomez, L., Sanders, E.A., Tabone, M.D., Plantaz, D., Etzioni, A., Monafo, V., Abinun, M., Hammarstrom, L., Abrahamsen, T., Jones, A., Finn, A., Klemola, T., DeVries, E., Sanal, O., Peitsch, M.C., Notarangelo, L.D., 1997. Clinical spectrum of X-linked hyper-IgM syndrome. J. Pediatr. 131, 47–54.

Li, L., Cao, D., Garber, D.W., Kim, H., Fukuchi, K., 2003. Association of aortic atherosclerosis with cerebral beta-amyloidosis and learning deficits in a mouse model of Alzheimer's disease. Am. J. Pathol. 163, 2155–2164.

Maier, M., Seabrook, T.J., Lemere, C.A., 2005. Modulation of the humoral and cellular immune response in Abeta immunotherapy by the adjuvants monophosphoryl lipid A (MPL), cholera toxin B subunit (CTB) and *E. coli* enterotoxin LT(R192G). Vaccine 23, 5149–5159.

Maier, M., Seabrook, T.J., Lazo, N.D., Jiang, L., Das, P., Janus, C., Lemere, C.A., 2006. Short amyloid-beta (Abeta) immunogens reduce cerebral Abeta load and learning deficits in an Alzheimer's disease mouse model in the absence of an Abeta-specific cellular immune response. J. Neurosci. 26, 4717–4728.

Monsonego, A., Maron, R., Zota, V., Selkoe, D.J., Weiner, H.L., 2001. Immune hyporesponsiveness to amyloid beta-peptide in amyloid precursor protein transgenic mice: implications for the pathogenesis and treatment of Alzheimer's disease. Proc. Natl. Acad. Sci. U. S. A. 98, 10273–10278.

Monsonego, A., Imitola, J., Zota, V., Oida, T., Weiner, H.L., 2003. Microglia-mediated nitric oxide cytotoxicity of T cells following amyloid beta-peptide presentation to Th1 cells. J. Immunol. 171, 2216–2224.

Nicoll, J.A., Wilkinson, D., Holmes, C., Steart, P., Markham, H., Weller, R.O., 2003. Neuropathology of human Alzheimer disease after immunization with amyloid-beta peptide: a case report. Nat. Med. 9, 448–452.

Nikolic, W.V., Bai, Y., Obregon, D., Hou, H., Mori, T., Zeng, J., Ehrhart, J., Shytle, R.D., Giunta, B., Morgan, D., Town, T., Tan, J., 2007. Transcutaneous beta-amyloid immunization reduces cerebral beta-amyloid deposits without T cell infiltration and microhemorrhage. Proc. Natl. Acad. Sci. U. S. A. 104, 2507–2512.

O'Keefe, G.M., Nguyen, V.T., Benveniste, E.N., 2002. Regulation and function of class II major histocompatibility complex, CD40, and B7 expression in macrophages and microglia: Implications in neurological diseases. J. Neurovirology 8, 496–512.

Okura, Y., Miyakoshi, A., Kohyama, K., Park, I.K., Staufenbiel, M., Matsumoto, Y., 2006. Nonviral Abeta DNA vaccine therapy against Alzheimer's disease: long-term effects and safety. Proc. Natl. Acad. Sci. U. S. A. 103, 9619–9624.

Orgogozo, J.M., Gilman, S., Dartigues, J.F., Laurent, B., Puel, M., Kirby, L.C., Jouanny, P., Dubois, B., Eisner, L., Flitman, S., Michel, B.F., Boada, M., Frank, A., Hock, C., 2003. Subacute meningoencephalitis in a subset of patients with AD after Abeta42 immunization. Neurology 61, 46–54.

Ponomarev, E.D., Shriver, L.P., Dittel, B.N., 2006. CD40 expression by microglial cells is required for their completion of a two-step activation process during central nervous system autoimmune inflammation. J. Immunol. 176, 1402–1410.

Rezai-Zadeh, K., Shytle, D., Sun, N., Mori, T., Hou, H., Jeanniton, D., Ehrhart, J., Townsend, K., Zeng, J., Morgan, D., Hardy, J., Town, T., Tan, J., 2005. Green tea epigallocatechin-3-gallate (EGCG) modulates amyloid precursor protein cleavage and reduces cerebral amyloidosis in Alzheimer transgenic mice. J. Neurosci. 25, 8807–8814.

Schenk, D.B., Yednock, T., 2002. The role of microglia in Alzheimer's disease: friend or foe? Neurobiol. Aging 23, 677–679 (discussion 683-4).

Schenk, D., Barbour, R., Dunn, W., Gordon, G., Grajeda, H., Guido, T., Hu, K., Huang, J., Johnson-Wood, K., Khan, K., Kholodenko, D., Lee, M., Liao, Z., Lieberburg, I., Motter, R., Mutter, L., Soriano, F., Shopp, G., Vasquez, N., Vandevert, C., Walker, S., Wogulis, M., Yednock, T., Games, D., Seubert, P., 1999. Immunization with amyloid-beta attenuates Alzheimer-disease-like pathology in the PDAPP mouse. Nature 400, 173–177.

Sigurdsson, E.M., Wisniewski, T., Frangione, B., 2002. A safer vaccine for Alzheimer's disease? Neurobiol. Aging 23, 1001–1008.

Straw, A.D., MacDonald, A.S., Denkers, E.Y., Pearce, E.J., 2003. CD154 plays a central role in regulating dendritic cell activation during infections that induce Th1 or Th2 responses. J. Immunol. 170, 727–734.

Tan, J., Town, T., Paris, D., Mori, T., Suo, Z., Crawford, F., Mattson, M.P., Flavell, R.A., Mullan, M., 1999. Microglial activation resulting from CD40–CD40L interaction after beta-amyloid stimulation. Science 286, 2352–2355.

Tan, J., Town, T., Mullan, M., 2000. CD45 inhibits CD40L-induced microglial activation via negative regulation of the Src/p44/42 MAPK pathway. J. Biol. Chem. 275, 37224–37231.

Tan, J., Town, T., Crawford, F., Mori, T., DelleDonne, A., Crescentini, R., Obregon, D., Flavell, R.A., Mullan, M.J., 2002. Role of CD40 ligand in amyloidosis in transgenic Alzheimer's mice. Nat. Neurosci. 5, 1288–1293.

Togo, T., Akiyama, H., Kondo, H., Ikeda, K., Kato, M., Iseki, E., Kosaka, K., 2000. Expression of CD40 in the brain of Alzheimer's disease and other neurological diseases. Brain Res. 885, 117–121.

Town, T., Tan, J., Mullan, M., 2001a. CD40 signaling and Alzheimer's disease pathogenesis. Neurochem. Int. 39, 371–380.

Town, T., Tan, J., Sansone, N., Obregon, D., Klein, T., Mullan, M., 2001b. Characterization of murine immunoglobulin G antibodies against human amyloid-beta1–42. Neurosci. Lett. 307, 101–104.

Town, T., Vendrame, M., Patel, A., Poetter, D., DelleDonne, A., Mori, T.,

Smeed, R., Crawford, F., Klein, T., Tan, J., Mullan, M., 2002. Reduced Th1 and enhanced Th2 immunity after immunization with Alzheimer's beta-amyloid(1–42). J. Neuroimmunol. 132, 49–59.

Town, T., Tan, J., Flavell, R.A., Mullan, M., 2005. T-cells in Alzheimer's disease. Neuromolecular Med. 7, 255–264.

Townsend, K.P., Town, T., Mori, T., Lue, L.F., Shytle, D., Sanberg, P.R., Morgan, D., Fernandez, F., Flavell, R.A., Tan, J., 2005. CD40 signaling regulates innate and adaptive activation of microglia in response to amyloid beta-peptide. Eur. J. Immunol. 35, 901–910.

van Kooten, C., Banchereau, J., 2000. CD40–CD40 ligand. J. Leukoc Biol. 67, 2–17.

Washington, R.A., Becher, B., Balabanov, R., Antel, J., Dore-Duffy, P., 1996. Expression of the activation marker urokinase plasminogen-activator receptor in cultured human central nervous system microglia. J. Neurosci. Res. 45, 392–399.

Wilcock, D.M., Rojiani, A., Rosenthal, A., Subbarao, S., Freeman, M.J., Gordon, M.N., Morgan, D., 2004. Passive immunotherapy against Abeta in aged APP-transgenic mice reverses cognitive deficits and depletes parenchymal amyloid deposits in spite of increased vascular amyloid and microhemorrhage. J. Neuroinflammation 1, 24.

Wilcock, D.M., Jantzen, P.T., Li, Q., Morgan, D., Gordon, M.N., 2007. Amyloid-beta vaccination, but not nitro-nonsteroidal anti-inflammatory drug treatment, increases vascular amyloid and microhemorrhage while both reduce parenchymal amyloid. Neuroscience 144, 950–960.